Schrödinger Cat States and their Metrological Power

Submitted By

Aruza Naeem

(Registration No: 00000429873)

A thesis submitted to the National University of Sciences and Technology, Islamabad,
in partial fulfillment of the requirements for the degree of

Master of Science in

Physics

Supervisor: **Prof. Dr. Shahid Iqbal**

Department of Physics
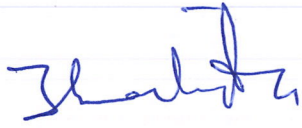
School of Natural Sciences

National University of Sciences and Technology (NUST)
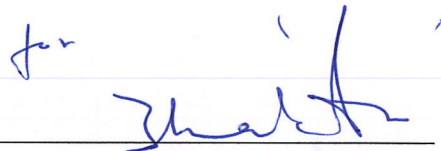
Islamabad, Pakistan

2022 - 2024

THESIS ACCEPTANCE CERTIFICATE

Certified that final copy of MS thesis written by **Aruza Naeem** (Registration No. **00000429873)**, of **School of Natural Sciences** has been vetted by undersigned, found complete in all respects as per NUST statutes/regulations, is free of plagiarism, errors, and mistakes and is accepted as partial fulfillment for award of MS/M.Phil degree. It is further certified that necessary amendments as pointed out by GEC members and external examiner of the scholar have also been incorporated in the said thesis.
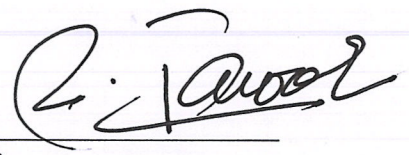
Signature: _____

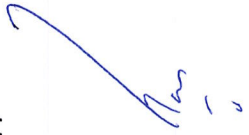Name of Supervisor: Prof. Shahid Iqbal

Date: _____ 12/8/2024 _____

Signature (HoD): _____

Date: _____ 12/8/2024 _____

Signature (Dean/Principal): _____

Date: _____ 12·08· 2024 _____

National University of Sciences & Technology

MS THESIS WORK

We hereby recommend that the dissertation prepared under our supervision by: Aruza Naeem, Regn No. 00000429873 Titled: Schrödinger Cat States and their Metrological Power be Accepted in partial fulfillment of the requirements for the award of **MS** degree.

Examination Committee Members

1. Name: DR. MUHAMMAD ALI PARACHA   Signature: _____

2. Name: DR. NAILA AMIR   Signature: _____

Supervisor's Name PROF. SHAHID IQBAL   Signature: _____

_____
Head of Department

12/8/2024.
Date

COUNTERSINGED

Date: 12·08·2024

Dean/Principal

To my parents, who made me what I am today.

ACKNOWLEDGEMENTS

Contents

List of Abbreviations

3H cat Three Headed Cat State. 21

4H Cat Four Headed Cat State. 22

CRB Cramer-Rao Bound. v, 44, 75

FI Fisher Information. 43

HD Homodyne Detection. 24

HL Heisenberg Limit. 5

MH Multiheaded Cat States. 21, 23

OPO Optical Parametric Oscillator. 24

ORM Operational Resource Measure. 49

ORT Operational Resource Theory. 49

PBS Polarized Beam Splitter. 24

PDF Probability Distribution Function. 27

POVM Positive Operator Valued Measurements. 43

QFI Quantum Fisher Information. v, 45, 78

RT Resource Theories. 48

SLD Symmetric Logarithmic Derivative. 44

List of Figures

Abstract

Schrödinger Cat States, which in quantum optics refer to a superposition of distinct coherent states, have acquired pedestal due to their application in quantum technologies. Despite the challenges involved, efforts are underway to generate large size cat states in the laboratories. Their importance in quantum metrology, in enhancing precision measurement is monumental.

This thesis explores the power these states hold in enhancing metrology for phase and displacement sensing. We begin by exploring the nonclassicality of cat states through Wigner function, then continue towards analyzing their photon statistics. We analytically studied as to whether Mandel Q parameter can serve as an indicator for relative strength of cat states, with coherent states as benchmark, for precisely measuring phase and displacement. Our results demonstrate that Q is not sufficient in dictating the metrological advantage of the cat states across different parameters. The study was extended to include various probe states with similar construction as Schrödinger cat states called as multiheaded cats. Next, we explore the impact of single photon addition on metrological power of all the states considered. Through graphical analysis, we elucidate that this manipulation of cat states result in further enhancing their metrological potential, as photon addition is a non-local operation and can add to the operational nonclassicality of a state.

Our findings underscore the significance of Schrödinger cat states and highlight the advantage of manipulation of photon number in enhancing quantum metrology.

Chapter 1

Introduction

1.1 Overview

The world of quantum mechanics, most of the time challenges our logic owing to its counter-intuitive nature. Quantum superposition and entanglement are quintessence of the strangeness associated with that world. This aspect can be exemplified by Schrödinger cat. In this chapter, we delve into the Schrödinger cat state, explore its potential applications in quantum technologies, introduce quantum metrology and present future research prospects.

1.2 Schrödinger Cat State

1.2.1 Historical Context

Schrödinger's cat is an eponym of Erwin Schrödinger. In 1935, Schrödinger through his paper titled "The Present Situation in Quantum Mechanics" (translated from German) [1] proposed a famous thought experiment involving a cat. The idea was put forth as a critique against Max Born's probabilistic interpretation of wave-function, which according to Schrödinger results in ridiculous cases where superposition at microscopic scale could get entangled with that of at macroscopic scale. The setup for Schrödinger's gedanken experiment , given in figure 1.2.1, illustrates a cat confined in a box along with a radioactive element and a vile of poison. The probability of decay of the radioactive element in one hour is half, which constitutes a superposition at microscopic level. If the element decays

within the given time it initiates a process by which the vile is hammered down and the cat being exposed to the poison dies and lives otherwise, constituting a superposition in macroscopic world. Any measurement on the system afterwards, represented by looking inside the box, will collapse the macroscopic superposition in either of the distinct states in fig. 1.2.1 (c) or (d). This cat that simultaneously exist in the box in alive and dead state is dubbed as a Schrödinger Cat.
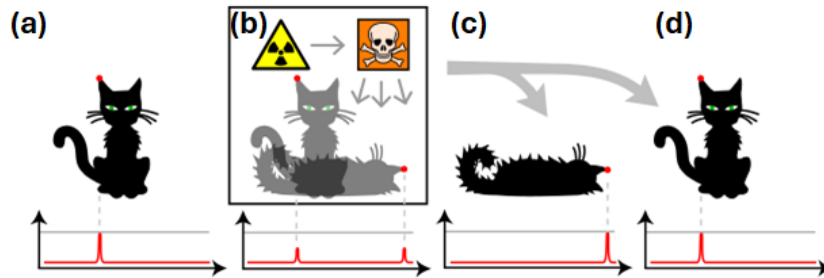
Figure 1.2.1: Schrödinger's Gedanken Experiment [2]

1.2.2 Timeline of Adoption of Schrödinger cat

"Schrödinger cat", though originally stood as a critique, the terminology was over the time adopted by the corpus of quantum mechanics. It now refers to a superposition of macroscopically distinct quantum states. The timeline is as under:

1935: Schrödinger introduces his namesake cat through the thought experiment.

1950-70s: The fundamental principles on which quantum mechanics stand were being vehemently debated by the scientists. In 1963, Glauber gave coherent states. The even and odd superposition of coherent states introduced by Dodonov et al., in 1973, in their seminal paper [3] were titled as even and odd coherent states respectively.

1980s: With advancement in quantum optics and technology, scientists were able to test the superpositions at quantum scale. In 1986, Yurke and Stoler introduced yet another superposition of coherent states as generalized coherent states. The states introduced are now referred to as Yurke-Stoler states and 4 headed cat state.

1990s: With the publication of Brune and Haroche [4] in 1992 on generation of Schrödinger cat state, the terminology began to appear more frequently in publications and depicted superposition of classical fields (coherent state).

2000s: The terminology gets rooted in vocabulary of quantum physics. Extensive experimental setups with an aim to generate, measure and manipulate the Schrödinger cat states further solidified the term.

1.2.3 Schrödinger Cats in Quantum Optics

A Schrödinger cat state (henceforth referred to as cat) is considered as a superposition of states which are macroscopically distinct. In quantum optics, superposition of two distinct classical fields, i.e., coherent state, is called a Schrödinger cat state. In phase space, an even cat can be visualised through a quasi-probability distribution function called as Wigner function.
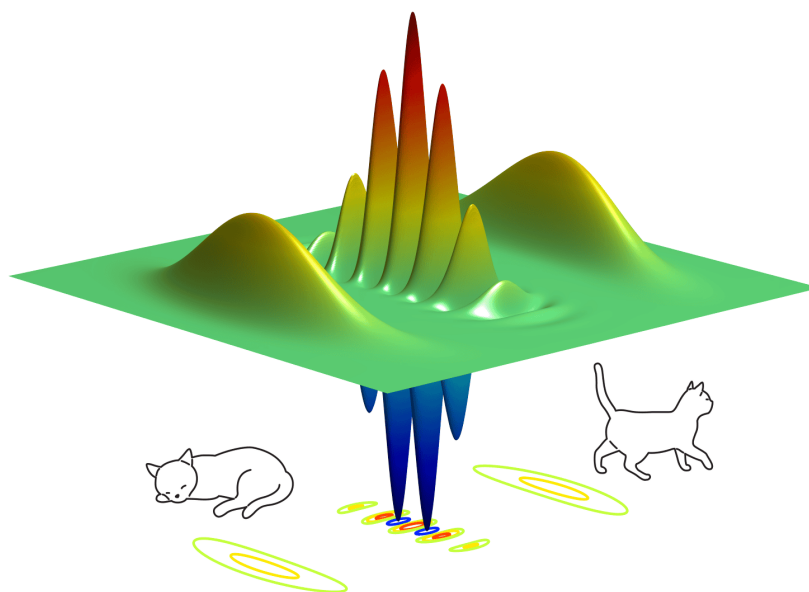
Figure 1.2.2: Phase Space Representation of Even Cat [5]

The two gaussian curves atop the central plane represent overlapping of similar classical fields, each denoted by a distinct state of a cat being alive or dead; whereas, the fringe pattern in between reflects overlapping of the two distinct states. The negative curves, which may astound the reader at first, hold extreme significance in quantum optics and will be discussed in chapter 3.

1.2.4 Creating Schrödinger Cats in Labs

Early efforts to create cats in the labs go as far back as 1992. However, after decades of research cats are being created utilizing various phenomena. Method of atom-field

interaction like trapping ion or photon in quantum cavity [4],[6] acts as precursor to various approaches like subtraction of photon methods [7],[8],[9],[10], and photon addition method [11]; however, all these methods fail to produce cats with large amplitude. The most recent approach that utilizes quantum Zeno effect and interaction free measurement [12] allows creating cats with relatively large amplitude.

1.2.5   Challenges to Schrödinger Cats

Though, the importance of cat states in quantum technology cannot be accentuated enough, there are certain challenges which do prevail and limit their utility: the challenges being scalability i.e. creating large amplitude optical cat states. Despite the best experimental efforts, α remains less than 2 [12], and owing to the fragility of cat states, they tend to decohere on interaction with environment.

1.2.6   Significance

Cat states show promise for understanding fundamental physics and various practical applications:

Fundamental Physics: Cat states help in navigating the quantum-classical boundary [13] . These are also utilized in testing the underpinnings of quantum mechanics [14].

Quantum Information: Cat states are versatile resources in quantum information processing. They play pivotal role in enabling quantum error correction [15], enhancing communication protocols [16], and can be utilized for creating complex quantum states [17].

Quantum Metrology: Cat states offer the potential to surpass classical limits in precision measurements. Their sensitivity to phase shifts and other parameters enable enhanced sensing capabilities in various applications such as atomic clocks [18], gravitational wave detectors and magnetic imaging making them versatile for material and medical science [19].

1.3   Quantum Metrology

Quantum metrology deals with studying ways to enhance precision and accuracy in measuring various physical parameters beyond classical limit, using principles of quantum

mechanics such as entanglement and superposition. Despite the fact that quantum mechanics imposes limit on precisely measuring complementary variables due to Heisenberg Uncertainty Principle, it also paves way for techniques in enhancing metrology. Quantum metrology began with the seminal paper of C. M. Caves [20] in which he proposed the "squeezed state" technique that illustrated how shot noise i.e., a quantum mechanical error associated with photon number fluctuations in interferometers could be reduced using quantum correlations. Techniques such as these become pertinent when precision cannot be enhanced by increase of optical power [21]. Mostly, the instruments employed for carrying out quantum metrology resemble those utilized for classical metrology. For example, interferometers when used with quantum states can help beat classical limit, which is called as Standard Quantum Limit (SQL) or Shot Noise, and approach Heisenberg Limit (HL).

1.3.1 Estimation Tasks in Quantum Metrology

Quantum metrology is carried out in three main steps: state preparation, parameter encoding, measurement along with classical estimation techniques [22] as shown in figure 4.1.1.
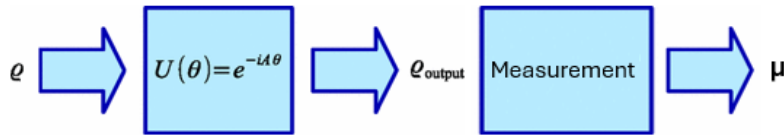
Figure 1.3.1: Tasks for Parameter Estimation in Quantum Metrology

Briefly, a classical parameter of interest is encoded on a probe state through a quantum map. The resulting state of the system is measured through application of generalized measurements which are chosen appropriately followed by techniques of data processing. In order to achieve optimal precision, all the elements of quantum metrology need to be optimized. This paper, analyzes the impact of optimizing the probe state from within the cats.

1.3.2 Enhancing Metrology with Cats

Schrödinger cat states, when used as probe states can lead to enhancing the sensitivity of measuring devices by using quantum interference. For example, in Mach Zehnder In-

terferometer, cat states can be used in reducing noise and increasing phase sensitivity, which results in measurements that beat SQL asymptotically; thus approaching Heisenberg limit [23], which is an ultimate quantum limit in precision.

1.4   Future Research

Future research directions include looking for ways to further enhancing the quantum metrology of cat states by exploiting entanglement and multiple photon addition.

1.5   Outline

This thesis has been organized as under:

Chapter 2 pertains to rudimentary concepts related to Glauber Coherent States which include the definition and discussion on their classical nature, properties and generating technique. The said discussion then naturally leads to exploring different forms of Schrödinger cats, Yurke-Stoler states, multiheaded cats and their excited counter-parts. In the end we have also produced a scheme for creating excited states in lab.

Chapter 3, we talk about the non-classicality and various quantifiers which capture the nonclassical nature of the states such as Wigner function and Mandel Q parameter. Wigner functions and Mandel Q parameter of the multiheaded cat states have been worked out.

Chapter 4, pertains to the various quantum tasks involved in parameter estimation through quantum metrology. Two operational quantifiers of nonclassicality have been reviewed, which includes metrological power of states and operational resource measure which serves as tight upper bound on the prior. The measure has been employed in later part to work out the metrological power for displacement sensing, followed by calculations for metrological power for phase sensing.

Chapter 5 deals with the analysis, through graphical comparison, as to whether Mandel Q parameter serves as an indicator of relative strength of metrological power irrespective of the parameter measured, or not. Furthermore, We have analyzed the impact of photon addition to cats on their photon statistics and in enhancing their metrological power.

Chapter 6   In this chapter we have presented the summary and conclusion of our work.

Appendix, detail calculations have been appended at the end, as they could have disrupted the flow of this document.

Chapter 2

Schrödinger Cat State in Quantum Optics

Schrödinger considered the possibility of existence of the cat, a classical object, in super-position of two distinct states i.e., alive and dead a "ridiculous case", which is a direct consequence of superposition at microscopic level. Quantum Optics, realizes such a cat by taking superposition of a classical entity with two distinct states that can be actuated with exclusiveness of an alive and dead cat, especially when that entity is "macroscopic" enough. This enigmatic entity is called a Coherent state. Coherent state is the most classical quantum state, as its dynamics resembles that of a classical system and the distinct forms can be obtained by controlling the phase of these states. However, the resulting Schrödinger cat is purely a quantum state as its a superposition of coherent states, and give rise to number of phenomena which have no classical analogue.

2.1   Coherent States

In chapter 1, we have already introduced the even cat; however, that is not the only possible combination of the coherent states with respect to their relative phases. We begin this chapter by putting forth the concept of coherent state. The reasons as to why these quantum states are dubbed as classical, what are their properties and how they can be generated have been explored. In the later part, we introduce the various forms of Schrödinger cat states and then extend our discussion towards generalized cats, followed by creation of excited cats.

2.1.1   Coherent States in Literature

Coherent states were first presented by Schrödinger, in 1926, as solution to Schrödinger equation. He showed them as wave packet for a large number of wave functions of harmonic oscillator. The significance of this wave packet was that it did not spread with respect to time [24]. Another interpretation of coherent states came as eigenstates of annihilation operator $\hat{a}$ from G. Iwata [25]. It was much later in 1963 when J. Glauber and E. C. G. Sudarshan (independently) systematically presented these states as superposition of the number states, the later forming a complete set [26],[27]; however, the name "coherent states" is attributed to Glauber alone.

2.1.2   Quantization of Cavity Field

The motivation that led Glauber to present coherent states as description of the field, with intrinsically uncertain number of photons, was the inadequacy of defined number state $|n\rangle$ in calculations involved in quantum electrodynamics. He equated the field states to that of states of quantum oscillator owing to the similarity between the Hamiltonian of the two, i.e., the Hamiltonian of field given by,

$$H = \frac{1}{2}\int dV\left[\varepsilon_o\mathbf{E}^2(\mathbf{r},t) + \frac{1}{\mu_o}\mathbf{B}^2(\mathbf{r},t)\right], \tag{2.1.1}$$

where, $\mathbf{E}$ and $\mathbf{B}$ are the single-mode cavity electric and magnetic fields are of following forms when polarization is considered along x-axis, and propagation of field along z-axis,

$$E_x(z,t) = \left(\frac{2\omega^2}{V\varepsilon_o}\right)^{1/2}q(t)\sin(kz), \tag{2.1.2}$$

$$B_y(z,t) = \frac{1}{c^2k}\left(\frac{2\omega^2}{V\varepsilon_o}\right)^{1/2}\frac{dq(t)}{dt}\cos(kz), \tag{2.1.3}$$

where, ω is the single mode frequency linked with wave number k through dispersion relation $\omega = ck$, V is the volume of the cavity and $q(t)$ is a time dependent quantity with length as dimension. Plugging above fields in eq. (2.1.1), and using orthogonality condition for trigonometric quadratures, we get,

$$H = \frac{1}{2}(p^2 + \omega^2 q^2),$$

which equates to the Hamiltonian of a simple harmonic oscillator with $m = 1$. The frequency of classical oscillations ω are associated with spring constant k through $k = m\omega^2$. Quantizing the system implies replacing the classical parameters with the quantum observables and introducing their commutators, thus,

$$\hat{E}_x(z,t) = \left(\frac{2\omega^2}{V\varepsilon_o}\right)^{1/2} \hat{q}\sin(kz), \tag{2.1.4}$$

$$\hat{B}_y(z,t) = \frac{1}{c^2 k}\left(\frac{2\omega^2}{V\varepsilon_o}\right)^{1/2} \hat{p}\cos(kz), \tag{2.1.5}$$

and,

$$\hat{H} = \frac{1}{2}(\hat{p}^2 + \omega^2\hat{q}^2), \tag{2.1.6}$$

$\hat{p}$ and $\hat{q}$ are hermitian complementary variables representing momentum and position operators respectively, with following commutator,

$$[\hat{q}, \hat{p}] = i\hbar. \tag{2.1.7}$$

Introducing two non-Hermitian operators, $\hat{a} := \frac{1}{\sqrt{2\hbar\omega}}(\omega\hat{q} + i\hat{p})$, $\hat{a}^\dagger := \frac{1}{\sqrt{2\hbar\omega}}(\omega\hat{q} - i\hat{p})$ and a Hermitian number operator $\hat{n}$ as $\hat{n} = \hat{a}^\dagger\hat{a}$, the Hamiltonian in eq. (2.1.6) becomes,

$$\hat{H} = \hbar\omega\left(\hat{n} + \frac{1}{2}\right). \tag{2.1.8}$$

The introduced operators follow the undermentioned commutation laws,

$$[\hat{a}, \hat{a}^\dagger] = 1, \quad [\hat{a}, \hat{n}] = \hat{a}, \text{ and } \quad [\hat{a}^\dagger, \hat{n}] = -\hat{a}^\dagger. \tag{2.1.9}$$

As, $\hat{n}$ and $\hat{H}$ commute, they are compatible observables and share an eigenket, obtained through diagonalization of the two, with corresponding eigenvalues n and E_n respectively,

$$\hat{H}|n\rangle = E_n|n\rangle, \quad \hat{n}|n\rangle = n|n\rangle, \tag{2.1.10}$$

where $|n\rangle$ can be referred as energy eigenstate of the cavity field. The non-Hermitian operators $\hat{a}$ and $\hat{a}^\dagger$ are called as annihilation and creation operator as when operated on the eigenstate, they result in annihilating and creating a quantum of energy $\hbar\omega$, respectively,

$$\hat{H}(\hat{a}|n\rangle) = (E_n - \hbar\omega)|n\rangle, \quad \hat{H}(\hat{a}^\dagger|n\rangle) = (E_n + \hbar\omega)|n\rangle. \tag{2.1.11}$$

An umbrella term used for these operators is ladder operators, as they cause addition or deletion a quanta from the number state,

$$\hat{a}|n\rangle = \sqrt{n}|n-1\rangle, \quad \hat{a}^\dagger|n\rangle = \sqrt{n+1}|n+1\rangle, \tag{2.1.12}$$

with $\hat{n}$ called as photon number operator giving the number of quanta or photons in the state,

$$\hat{a}^\dagger\hat{a}|n\rangle = n|n\rangle, \tag{2.1.13}$$

where, $n = 0, 1, 2, 3...$, a consequence of normalization condition for $\hat{a}|n\rangle$. All the higher number states can be generated by repeated application of creation operator on vacuum, where vacuum is the lowest number state attainable,

$$|n\rangle = \frac{(\hat{a}^\dagger)^n}{\sqrt{n!}}|0\rangle, \quad \hat{a}|0\rangle = 0. \tag{2.1.14}$$

As $|n\rangle$ are eigenstates of Hermitian operators; therefore, they ought to be orthonormal, satisfying following conditions,

$$\sum_m |n\rangle\langle n| = 1, \quad \langle n|m\rangle = \delta_{n,m}. \tag{2.1.15}$$

Number states can thus be used as basis, i.e., any state and operator can be expresses in terms of these states. Even though this basis set present descriptions of field with definite energy E_n and n photons, these are not the eigenstates of the field itself as $\langle n|E_x(r,t)|n\rangle = 0$.

11

2.1.3   Glauber Coherent State

Glauber defined single mode coherent states as eigenstates of annihilation operator satisfying following equation [26],

$$\hat{a}|\alpha\rangle = \alpha|\alpha\rangle. \tag{2.1.16}$$

Since, $\hat{a}$ and $\hat{a}^\dagger$ are non-hermitian operators, the eigenvalue α is a complex number. As, energy eigenstates of the harmonic oscillator or number states are orthonormal, coherent states can be expanded with number states as basis,

$$|\alpha\rangle = \sum_{n=0}^{\infty} C_n|n\rangle, \tag{2.1.17}$$

where, C_n's are the expansion co-efficients. Eq. (2.1.16) together with Eq. (2.1.17) yield,

$$C_n = \langle n|\alpha\rangle = e^{-|\alpha|^2/2}\frac{\alpha^n}{\sqrt{n!}}$$
$$\Rightarrow |\alpha\rangle = e^{-|\alpha|^2/2}\sum_{n=0}^{\infty}\frac{\alpha^n}{\sqrt{n!}}|n\rangle. \tag{2.1.18}$$

Significance of α

The significance of α becomes evident by taking expectation value of the number operator,

$$\langle\hat{n}\rangle = \langle\alpha|\hat{a}^\dagger\hat{a}|\alpha\rangle = |\alpha|^2, \tag{2.1.19}$$

thus, for the states unlike number states where number of photons is not definite $\langle\hat{n}\rangle$ gives the average number of photons, and for coherent states $|\alpha|^2$ takes the meaning of average number of photons in the field. The fluctuations in the photon number given by $\Delta\hat{n}^2$ is given as under,

$$\langle(\Delta\hat{n})^2\rangle = \langle\hat{n}^2\rangle - \langle\hat{n}\rangle^2,$$
$$= \langle\alpha|\hat{a}^\dagger\hat{a}\hat{a}^\dagger\hat{a}|\alpha\rangle - (\langle\alpha|\hat{a}^\dagger\hat{a}|\alpha\rangle)^2,$$

using the commutator relation $[\hat{a}, \hat{a}^\dagger] = 1$,

$$= |\alpha|^2. \tag{2.1.20}$$

As, average number of photons and its fluctuations in field is same, the photon statistics in the field are Poissonian. A fact, reinforced through probability of finding n photons in the state,

$$
\begin{aligned}
P_n &= |\langle n|\alpha\rangle|^2, \\
&= (e^{-|\alpha|^2/2})^2 \frac{(\alpha\alpha^*)^n}{n!}, \\
&= e^{-|\alpha|^2} \frac{|\alpha|^{2n}}{n!},
\end{aligned} \tag{2.1.21}
$$

which is a Poissonian profile.

Quantized Field States

Coherent states offer the description of electric field component of the light. Using eq. (2.1.4), and time dependent ladder operators, (obtained via Heisenberg equation of motion $d\hat{O}/dt = (i/\hbar)[\hat{H}, \hat{O}]$ used in Heisenberg picture, discussed in next subsection, to study evolution of operators),

$$E_x(z, t) = E_o(\hat{a}e^{-i\omega t} + \hat{a}^\dagger e^{i\omega t})\sin(kz), \tag{2.1.22}$$

taking expectation value with respect to coherent states,

$$\langle\alpha|E_x(z, t)|\alpha\rangle = E_o|\alpha|(e^{i(\theta-\omega t)} + e^{-i(\theta-\omega t)})\sin(kz), \tag{2.1.23}$$

$$= 2E_o|\alpha|\cos(\theta - \omega t)\sin(kz), \tag{2.1.24}$$

$$\neq 0. \tag{2.1.25}$$

2.1.4   Coherent State as Classical Field

Coherent states of the oscillator, are purely quantum in construction owing to be defined through superposition of number states, and thus use of term classical light to represent them is a misnomer. However, we can argue that these states have certain properties

which bring them closest to classical systems. In this sense, i.e., from quantum mechanical point of view, coherent states are dubbed as classical [28].

Minimum Uncertainty States

In Classical Mechanics, description of various systems through phase space helps in visualising the trajectories that system takes. The position and momentum coordinates of a point in phase space, give complete description of the system and can exactly be measured. When considered in the context for light, this entails measuring the amplitude and phase of electric field precisely. In contrast, the phase space description of a state in quantum mechanics is troublesome as all quantum states follow Heisenberg Uncertainty Principle. The principle dictates that complementary variables cannot be measured precisely, as for any such variables $\hat{R}$ and $\hat{T}$,

$$\langle(\Delta\hat{R})^2\rangle\langle(\Delta\hat{T})^2\rangle \geq \frac{1}{4}|\langle[\hat{R},\hat{T}]\rangle|^2. \tag{2.1.26}$$

Thus, if coherent states minimize this uncertainty i.e., allow system to be described in phase space nearest to trajectory of point particle, then they qualify as classical like. Rescaling position and momentum operators to dimensionless quadrature operators,

$$\hat{X}_\mu = \frac{i}{2}(e^{-i\mu}\hat{a}^\dagger - e^{i\mu}\hat{a}), \tag{2.1.27}$$

with $\mu = 0, \pi/2$ representing rescaled momentum and position operators, respectively. They are called as quadrature operators as in phase space they reveal the coherent state to be oscillating out of phase by 90°,

$$\langle\hat{X}_{\pi/2}\rangle = \frac{1}{2}(\alpha + \alpha^*) = |\alpha|\cos\theta = \text{Re}(\alpha), \tag{2.1.28}$$

$$\langle\hat{X}_0\rangle = \frac{i}{2}(\alpha^* - \alpha) = |\alpha|\sin\theta = \Im(\alpha). \tag{2.1.29}$$

Eq. (2.1.26) for quadrature operators becomes,

$$\langle(\Delta\hat{X}_{\pi/2})^2\rangle\langle(\Delta\hat{X}_0)^2\rangle \geq \frac{1}{4}|\langle[\hat{X}_{\pi/2},\hat{X}_0]\rangle|^2,$$
$$= \frac{1}{16}, \tag{2.1.30}$$

as $[\hat{X}_{\pi/2}, \hat{X}_0] = \frac{i}{2}$. The variance in each quadrature with respect to coherent state turns out to be equal,

$$\langle\alpha|(\Delta\hat{X}_{\pi/2})^2|\alpha\rangle = \frac{1}{4} = \langle\alpha|(\Delta\hat{X}_0)^2|\alpha\rangle, \tag{2.1.31}$$

with,

$$\langle\alpha|(\Delta\hat{X}_{\pi/2})^2|\alpha\rangle\langle\alpha|(\Delta\hat{X}_0)^2|\alpha\rangle = \frac{1}{16}. \tag{2.1.32}$$

Hence, coherent states are minimum uncertainty states and thus are most classical among all quantum states. The phase space depiction of coherent states is given in following fig. 2.1.1:

(a) Coherent state for small α **(b)** Coherent state for large α
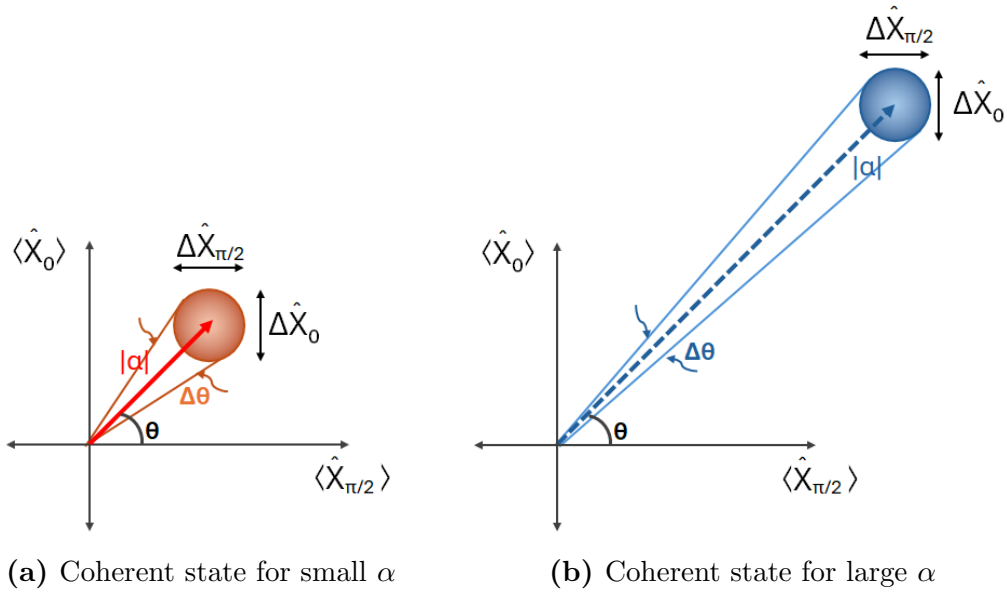
Figure 2.1.1: Phase space representation of a coherent state α with amplitude $|\alpha|$ and angle θ. Comparison of (a) and (b) depicts that in classical limit the phase uncertainty $\Delta\theta$ gets small, but quadrature uncertainty indicated by the shaded circle remains same

Classical Dynamics of Coherent State

The evolution of any state can be discerned by using the unitary time evolution operator $\hat{U} = e^{-\frac{i}{\hbar}\hat{H}t}$. Quantum systems for which the Hamiltonian are time independent, two evolution pictures can be used to govern their dynamics depending on whether the state or operator evolves; Schrödinger and Heisenberg picture. Schrödinger Picture (SP) dictates that the states evolve with time whereas the operator stays stationary and vice-versa for the Heisenberg picture. Using SP,

$$|\alpha(t)\rangle = \hat{U}|\alpha(0)\rangle,$$

using Hamiltonian of quantum harmonic oscillator,

$$= e^{-|\alpha|^2/2} \sum_n \frac{\alpha^n}{\sqrt{n!}} e^{-i\omega t(\hat{n}+1/2)} |n\rangle,$$

$$= e^{-i\omega t/2} e^{-|\alpha|^2/2} \sum_n \frac{(\alpha e^{-i\omega t})^n}{\sqrt{n!}} |n\rangle,$$

$$= e^{-i\omega t/2} |\alpha e^{-i\omega t}\rangle, \tag{2.1.33}$$

which shows that $|\alpha\rangle$ continues to stay as a coherent state, as it evolves with time.

Now let's look into the wave function of coherent state and the dynamics of its centroid:

$$\psi_\alpha(q) = \langle q|\alpha\rangle, \tag{2.1.34}$$

using definition of coherent state,

$$= e^{-|\alpha|^2/2} \sum_{n=0}^{\infty} \frac{\alpha^n}{\sqrt{n!}} \langle q|n\rangle, \tag{2.1.35}$$

using expression for number state wave function,

$$= e^{-\|\alpha\|^2/2} \sum_{n=0}^{\infty} \frac{\alpha^n}{\sqrt{n!}} \left[(2^n n!)^{-1/2} \left(\frac{\omega}{\pi\hbar}\right)^{1/4} e^{-\eta^2/2} H_n(\eta) \right], \tag{2.1.36}$$

where, $H_n(\eta)$ are the Hermite polynomial and $\eta = q\sqrt{\omega/\hbar}$. Using Hermite polynomial's generating function, $g(\eta, x) = e^{-x^2+2x\eta} = \sum_{m=0}^{\infty} (x^n/n!) H_n(\eta)$,

$$= \left(\frac{\omega}{\pi\hbar}\right)^{1/4} e^{-|\alpha|^2/2} e^{-\eta^2/2} \sum_{n=0}^{\infty} \frac{1}{n!} \left(\frac{\alpha}{\sqrt{2}}\right)^n H_n(\eta), \tag{2.1.37}$$

$$= \left(\frac{\omega}{\pi\hbar}\right)^{1/4} e^{-|\alpha|^2/2} e^{-\eta^2/2} e^{-\frac{\alpha^2}{2}+\sqrt{2}\alpha\eta}, \tag{2.1.38}$$

completing the square,

$$= \left(\frac{\omega}{\pi\hbar}\right)^{1/4} e^{-|\alpha|^2/2} e^{\eta^2/2} e^{-(\eta-\frac{\alpha}{\sqrt{2}})^2}, \tag{2.1.39}$$

this is a Gaussian wave function. The probability density with respect to position becomes,

$$= \left(\frac{\omega}{\pi\hbar}\right)^{1/2} e^{-|\alpha|^2} e^{\eta^2} e^{-(\sqrt{2}\eta-\alpha)^2}, \tag{2.1.40}$$

which is also a Gaussian. Similarly, the corresponding time evolved wave function is,

$$= \left(\frac{\omega}{\pi\hbar}\right)^{1/4} e^{-|\alpha|^2/2} e^{\eta^2/2} e^{-(\eta-\frac{\alpha e^{-i\omega t}}{\sqrt{2}})^2}, \tag{2.1.41}$$

with the probability density given as,

$$= \left(\frac{\omega}{\pi\hbar}\right)^{1/2} e^{-|\alpha|^2} e^{\eta^2} e^{-(\eta-\frac{\alpha e^{-i\omega t}}{\sqrt{2}})^2} e^{-(\eta-\frac{\alpha^* e^{i\omega t}}{\sqrt{2}})^2}, \tag{2.1.42}$$

$$= \left(\frac{\omega}{\pi\hbar}\right)^{1/2} e^{-(\eta-\sqrt{2}\Re\alpha e^{-i\omega t})^2}, \tag{2.1.43}$$

this is just an oscillatory Gaussian wave packet at all times. This is a signature classical behaviour, with a particle substituted by a wave packet. In contrast, other quantum mechanical states show dispersion with time. Looking at the centroid of the time evolved wave function,

$$\langle \hat{q} \rangle_t = \langle \alpha e^{-i\omega t} | \hat{q} | \alpha e^{-i\omega t} \rangle = \sqrt{\frac{\hbar}{2\omega}} \langle \alpha e^{-i\omega t} | \hat{a} + \hat{a}^\dagger | \alpha e^{-i\omega t} \rangle, \tag{2.1.44}$$

where, we have used $\hat{q} = \sqrt{\frac{\hbar}{2\omega}}(\hat{a} + \hat{a}^\dagger)$,

$$= \sqrt{\frac{\hbar}{2\omega}} e^{-|\alpha|^2} \sum_{m=0}^{\infty} \sum_{n=0}^{\infty} \frac{(\alpha e^{-i\omega t})^{*m}}{\sqrt{m!}} \langle m | \hat{a} + \hat{a}^\dagger | n \rangle \frac{(\alpha e^{-i\omega t})^n}{\sqrt{n!}}, \tag{2.1.45}$$

$$= \sqrt{\frac{\hbar}{2\omega}} e^{-|\alpha|^2} \sum_{m=0}^{\infty} \sum_{n=1}^{\infty} \frac{(\alpha e^{-i\omega t})^{*m}}{\sqrt{m!}} (\sqrt{n}\delta_{m,n-1} + \sqrt{n+1}\delta_{m,n+1}) \frac{(\alpha e^{-i\omega t})^n}{\sqrt{n!}}, \tag{2.1.46}$$

$$= \sqrt{\frac{\hbar}{2\omega}} e^{-|\alpha|^2} \sum_{m=0}^{\infty} \frac{|\alpha|^{2m}}{m!} |\alpha| (e^{i(\theta-\omega t)} + e^{-i(\theta-\omega t)}), \tag{2.1.47}$$

$$= \sqrt{\frac{2\hbar}{\omega}} \mathrm{Re}(\alpha e^{i\omega t}). \tag{2.1.48}$$

Similarly, for $\hat{p} = i\sqrt{\frac{\hbar\omega}{2}}(\hat{a}^\dagger - \hat{a})$,

$$\langle\hat{p}\rangle_t = \sqrt{2\hbar\omega}\,\text{Im}(\alpha e^{i\omega t}). \tag{2.1.49}$$

The above time average values of displacement and momentum operators, reflect oscillatory behaviour of the centroid of wave function of coherent state.

2.1.5 Properties of Coherent States

Prior to Glauber formalism for the coherent states, they were given no heed as they could not be used as basis. However, Glauber did explicitly showed a way in which operators and states could be expanded in terms of coherent states, bearing unique properties.

Non-orthogonality

Although coherent states are considered as classical, they cannot be distinguished if their amplitude is relatively small. This can be made evident by overlapping the two different coherent states $|\gamma\rangle$ and $|\lambda\rangle$ (for detail calculations refer to appendix A.1),

$$\begin{aligned}
\langle\lambda|\gamma\rangle &= (e^{-|\lambda|^2/2}\sum_{m=0}^{\infty}\frac{\lambda^{*m}}{\sqrt{m!}}\langle m|)(e^{-|\gamma|^2/2}\sum_{n=0}^{\infty}\frac{\gamma^n}{\sqrt{n!}}|n\rangle), \\
&= e^{-(|\lambda|^2+|\gamma|^2)/2}e^{\lambda^*\gamma}, \\
&= e^{-(|\lambda-\gamma|)^2/2}e^{(\lambda^*\gamma-\lambda\gamma^*)/2},
\end{aligned} \tag{2.1.50}$$

$$|\langle\lambda|\gamma\rangle|^2 = e^{-(|\lambda-\gamma|)^2}. \tag{2.1.51}$$

Hence, coherent states are not distinguishable unless $|\lambda - \gamma| \geq 0$, making them generally non-orthogonal [12] and [27].

Normalization

The coherent states are normalized, with their over-completeness [27] relation given as,

$$\int|\lambda\rangle\langle\lambda|\frac{d^2\lambda}{\pi} = 1, \tag{2.1.52}$$

(refer to appendix A.2) where, the integrand is integrated over the complex plane, $d^2\lambda = d(\Re\lambda)d(\Im\lambda)$.

2.1.6 Generating Coherent States

Generation of coherent states can be achieved by application of the unitary displacement operator $\hat{D}$ on vacuum state. The operator is a function of complex variable λ and is defined as under [26],

$$\hat{D}(\lambda) := e^{\lambda\hat{a}^\dagger - \lambda^*\hat{a}}, \tag{2.1.53}$$

when applied to vacuum state leads to,

$$|\lambda\rangle = D(\lambda)|0\rangle = e^{\lambda\hat{a}^\dagger - \lambda^*\hat{a}}|0\rangle. \tag{2.1.54}$$

The proof is given in appendix A.3

2.2 Schrödinger Cat States

A Schrödinger cat in quantum optics, as noted earlier, is defined as a superposition of macroscopically distinct $|\alpha\rangle$ and $|-\alpha\rangle$ coherent states, which is directly related to Schrödinger thought experiment where the macroscopic object, i.e. a cat (here actuated to coherent state being treated as classical state) is in superposition of classically distinct states, i.e. alive and dead (corresponds to $|\alpha\rangle$ and $|-\alpha\rangle$). Depending on the relative phase of the coherent states involved, in the said superposition; they can be classified as even or odd Schrödinger cats. Dodonov et al. mentioned the explicit form of these cats [3] as earliest as 1973, and tagged them as even and odd coherent states.

Even $|\psi_e\rangle$ and odd cats $|\psi_o\rangle$ are even and odd superposition of $|\alpha\rangle$ and $|-\alpha\rangle$, i.e., out of phase (distinct) coherent states with fixed phase difference of 0,

$$|\psi_e\rangle = N_e(|\alpha\rangle + |-\alpha\rangle), \tag{2.2.1}$$

(with $N_e = (2 + 2e^{-2|\alpha|^2})^{-1/2}$), and π,

$$|\psi_o\rangle = N_o(|\alpha\rangle - |-\alpha\rangle), \tag{2.2.2}$$

(with $N_o = (2 - 2e^{-2|\alpha|^2})^{-1/2}$), respectively, making them symmetric and anti-symmetric

under parity transformation ($\alpha \to -\alpha$). N_e and N_o represent constants obtained through normalization requirement of cats $\langle \psi | \psi \rangle$. The two distinct states can be visualized in phase space as depicted in fig. 2.2.1; however, the even cats, in literature, generally consider the coherent states on real line with $\theta = 0$ i.e., real α. This simplifies the mathematical analysis and graphical representation. Visualizing cats in phase space requires much more novel functions like Wigner function (discussed in the next chapter).
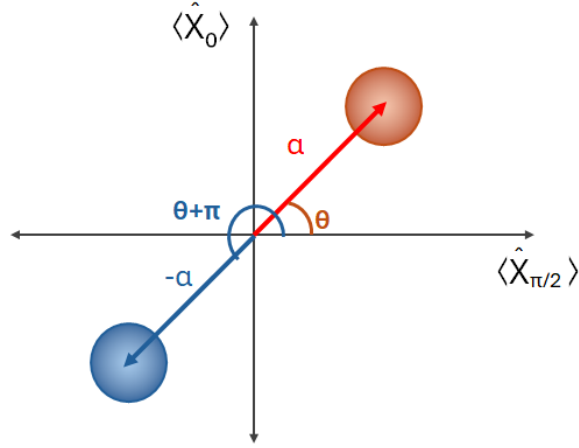
Figure 2.2.1: Phase space representation of two distinct forms of coherent states, which become completely distinguishable for large α.

It is pertinent to mention here that as coherent states are non-orthogonal, they cannot be said as distinct or distinguishable states in the strict sense of quantum mechanics, unless α is considered as very large causing the overlap of the two states $\langle \alpha | -\alpha \rangle = e^{-2|\alpha|^2}$ to vanish. However, the term distinct is employed as the difference between the two coherent states can be significant on macroscopic scale. Even though the classical states within the cats are not distinct at quantum level, the cats themselves enjoy orthogonality among them, and form complete sets separately in Hilbert space of even and off cats i.e.,

$$\langle \psi_e | \psi_o \rangle = 0, \quad \int |\psi_k\rangle\langle\psi_k| \frac{d^2\alpha}{\pi} = 1, \tag{2.2.3}$$

where $\quad i = e, o$.

The non-orthogonality of coherent states give rise to interference effects which is quintessence of superposition. It is due to this feature that cats find wide ranging applications in quantum technologies.

2.2.1 Yurke-Stoler State

Yurke-Stoler State (YS) presented by Yurke and Stoler [29] is also a superposition of the two distinct coherent states; however, there is an additional phase shift of $e^{i\pi/2}$ between them in the superposition unlike Schrödinger cats and are therefore not considered under the umbrella term. This phase shift gives rise to interference effects which are not in consonance with the cats (discussed in detail in next chapter). Mathematically, they are represented as under [30],

$$|\psi_{ys}\rangle = \frac{1}{\sqrt{2}}(|\alpha\rangle + i|-\alpha\rangle). \tag{2.2.4}$$

The unique interference pattern of YS demands it utility in experiments where more control over phase difference and coherence is needed.

2.2.2 Generalized Coherent or Multiheaded Cat States

In literature, there exist states which are superposition of more than two distinct coherent states, which can be considered as extension of cats. However, the nomenclature associated with them varies. For instance, Goldberg and Heshami dubs them as generalized cat states [31]. Lan et al. [32], introduces multiheaded quantum states, with N-headed coherent superposition state i.e., NHCSS in which N number of coherent states having equal weights are superposed, and Schrödinger cats are considered as quantum optics analogue of 2HCSS. These states are later on also termed as higher order cat states. Wenchao and Zubairy [33] have worked with superposition of three and four coherent states for analyzing their nonclassicality and have called them as three-headed and four-headed respectively. It is this later nomenclature that we are using in this document, with an umbrella term Multiheaded Cat States (MH) referring to superposition of M number of coherent states and by this classification Schrödinger cats and YS state can be considered as 2H cats. There are various forms of MH cats depending on their relative phases, the one considered in this document are discussed below.

Three Headed Cat State

Three Headed Cat State (3H cat) is generally a superposition of three distinct coherent states; however, we have taken the form in which two of the three states are coherent

with the third replaced by vacuum [33],

$$|\psi_{3h}\rangle = N_{3h}(|\alpha\rangle + |0\rangle + |-\alpha\rangle), \tag{2.2.5}$$

where, $N_{3h} = (3 + 4e^{-|\alpha|^2/2} + 2e^{-2|\alpha|^2})^{-1/2}$ is the normalization constant with significant contribution due to overlap of various states involved. The presence of third state in the superposition results in very unique properties different from cats. It may be pertinent to mention here that the coherent state $|\alpha = 0\rangle$ correspond to the oscillator's ground state, i.e., $|n = 0\rangle$, also called as vacuum. For vacuum state, number of photon is completely known, rendering the phase completely uncertain. In phase space, the three states can be visualized as follows,
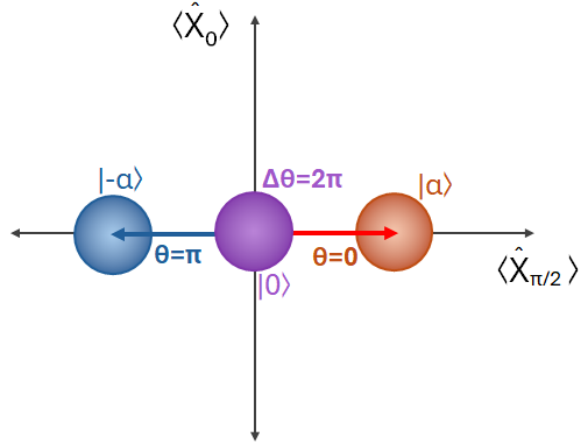
Figure 2.2.2: Phase space representation of three distinct forms of coherent states, with one coherent state replaced by vacuum. $\Delta\theta = 2\pi$ shows that the phase is completely uncertain.

Four Headed Cat State

Four Headed Cat State (4H Cat), as the name suggests, is formed by superposition of four coherent states with different phases.

$$|\psi_{4h}\rangle = \frac{1}{2}(|\alpha\rangle - |i\alpha\rangle + |-\alpha\rangle + |-i\alpha\rangle). \tag{2.2.6}$$

The form shared above was first explored by Yurke and Stoler [29], and has several significant features. The state is balanced superposition of four distinct coherent states symmetrically placed around the origin in phase space at $\theta = 0, \pi/2, \pi$ and $3\pi/2$. 4H Cat reveal complex interference patterns.
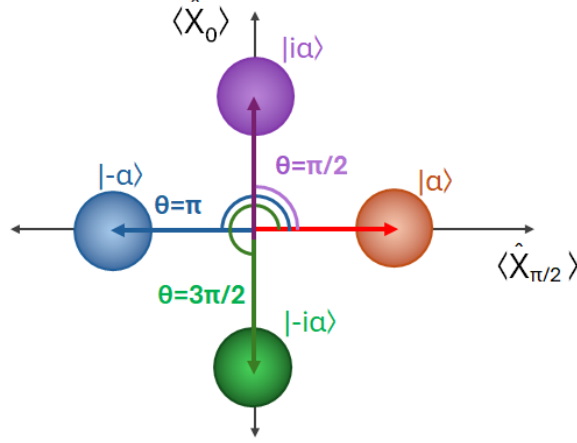
Figure 2.2.3: Phase space representation of four distinct forms of coherent states, symmetrically placed around origin.

MH, with M representing the number of coherent states involved in the superposition, are eigenstates of $\hat{a}^M$ with α^M as the eigenvalue,

$$\hat{a}^M|\psi_{Mh}\rangle = \alpha^M|\psi_{Mh}\rangle, \tag{2.2.7}$$

where, $|\psi_{Mh}\rangle$ represent an M headed cat.

2.2.3 Some Excited Multiheaded Cats

The single photon added cats can simply be prepared by application of the creation operator $\hat{a}^\dagger$ on the cats, Schrödinger as well as multiheaded [34], [35]. In this thesis, we have identified the photon added cats as excited cats. Table 2.1 shows all the excited multiheaded cats, which have been proposed by applying creation operator to their non-excited counterparts and then finding their respective normalization constant. N_{xyz} represent these constants obtained as, $\langle\psi_{xyz}|\psi_{xyz}\rangle = 1$.

Excited Cats	$|\psi_{xyz}\rangle$	N_{xyz}
Even	$|\psi_{eec}\rangle = N_{eec}\hat{a}^\dagger|\psi_e\rangle$	$N_{eec} = (1 + |\alpha|^2 \frac{N_e^2}{N_o^2})^{-1/2}$
Odd	$|\psi_{eoc}\rangle = N_{eoc}\hat{a}^\dagger|\psi_o\rangle$	$N_{eoc} = (1 + |\alpha|^2 \frac{N_o^2}{N_e^2})^{-1/2}$
YS	$|\psi_{eys}\rangle = N_{eys}\hat{a}^\dagger|\psi_{ys}\rangle$	$N_{eys} = (1 + |\alpha|^2)^{-1/2}$
3H	$|\psi_{e3h}\rangle = N_{e3h}\hat{a}^\dagger|\psi_{3h}\rangle$	$N_{e3h} = (1 + |\alpha|^2 \frac{N_{3h}^2}{N_o^2})^{-1/2}$
4H	$|\psi_{e4h}\rangle = N_{e4h}\hat{a}^\dagger|\psi_{4h}\rangle$	$N_{e4h} = \left(1 + |\alpha|^2\right)^{-1/2}$

Table 2.1: Excited Cats

2.2.4 Generating Excited Cats in Lab

Following the photon addition scheme to a coherent state given by Zavatta et al. [36], and Chen at al. [37], we have proposed following schematic for creation of excited cats.

Creation of Schrödinger Cat A laser source, which represents a coherent state created through stimulated emission, is used to first create a squeezed vacuum state in signal mode by passing the laser light through Optical Parametric Oscillator (OPO). The resulting state can be represented as $|\zeta\rangle_s|0\rangle_i$, where, $|\ \ \rangle_s$ and $|\ \ \rangle_i$ represent a signal and idler mode respectively. This state is then directed onto a beam-splitter, to produce a cat by photon subtraction [38]. The BS splits the beam into reflected and transmitted part, with non-zero probability of a photon being detected by Single Photon Detector (SPD). Thus, if the photon is detected in SPD, this means that it has been subtracted from the reflected beam, giving rise to $\hat{a}_s|\zeta\rangle_s|1\rangle_i$, where $\hat{a}_s|\zeta\rangle_s := |\psi_s\rangle_s$ is a cat in signal mode.

Photon Addition to Schrödinger Cat through SPDC Once the photon has been detected at the SPD the resulting state becomes $|\psi_s\rangle_s|0\rangle_i$. The beam is directed to Spontaneous Parametric Down Conversion (SPDC) where a pump beam is used to probabilistically add single photons to both signal and idler modes as under,

$$|\psi_f\rangle = (1 + g\hat{a}_s^\dagger\hat{a}_i^\dagger)|\psi_s\rangle_s|0\rangle_i = |\psi_s\rangle_s|0\rangle_i + g\hat{a}_s^\dagger|\psi_s\rangle_s|i\rangle_i, \qquad (2.2.8)$$

where, g is the gain factor of the SPDC process and $\hat{a}_s^\dagger|\psi_s\rangle_s$ is an excited cat in signal mode. SPDC basically annihilates a pump photon and creates an entangled photon pair in signal and idler mode [39], and the second term in above equation represents the probabilistic nature of creation of such a photon pair. The resulting beam advances to a Polarized Beam Splitter (PBS), which splits the resulting beam according to their polarization, as a type-II SPDC generates beams with orthogonal polarization. The idler mode photon goes to SPD and heralds or announces the arrival of excited cat to the Homodyne Detection (HD).

Homodyne Detection using the Generated Cat as Local Oscillator A part of the cat state generated is directed to the HD as a local oscillator i.e. a reference state, with which the excited cat is interfered at a BS. Homodyne detection allows observation of quadratures of cat state generated in the signal mode [40].
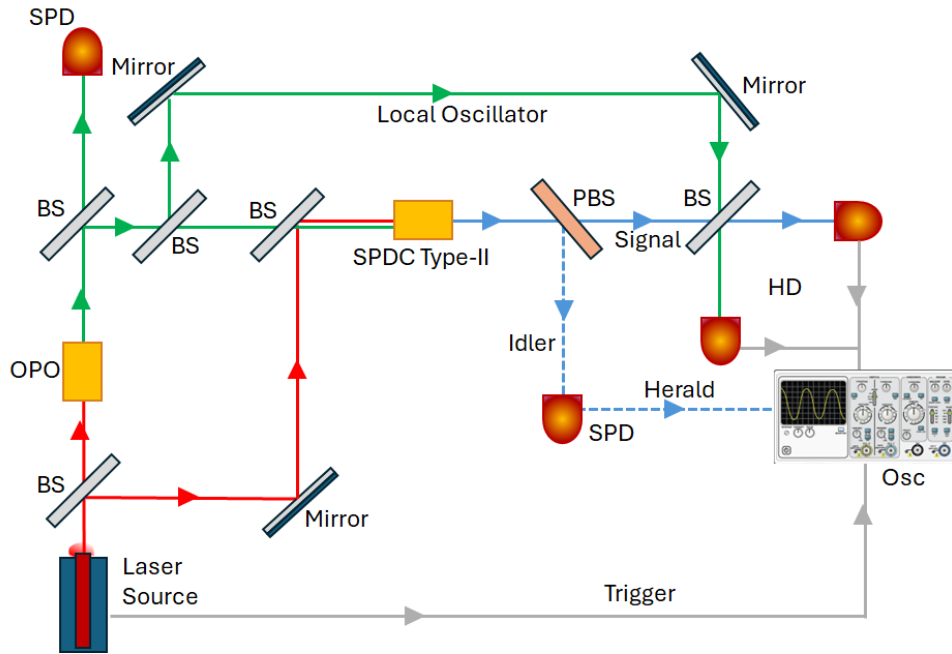
Figure 2.2.4: Schematics for creation of excited cat. The OPO generates squeezed vacuum state, which through photon subtraction creates cat state. Photon addition to cat and idler vacuum mode is ensured in SPDC. The idler photon heralds the signal mode to homodyne detector. Local oscillator (cat) and excited cats are made to interfere on beam-splitter for extraction of phase information by HD.

Chapter 3

Quantifying Nonclassicality of Schrödinger Cats

Nonclassicality of quantum states is generally defined as properties of states that cannot be described by classical physics. Such properties, may include entanglement, superposition and squeezing etc. In quantum technology, nonclassicality offers quantum advantage that has no classical analogue. Therefore, it is necessary to look for quantifiers of nonclassicality which could capture its extent in states. We open this chapter with the discussion on the criteria that quantum states ought to fulfill to be tagged as nonclassical, followed by discussion on some quantifiers of nonclassicality. In the end, the same quantifiers are used to explore the nature of multiheaded cats.

3.1 Nonclassicality and P Function

P Representation of Coherent States

The density operator representing the state can be expanded in terms of coherent states as,

$$\hat{\rho} = \int P(\alpha)|\alpha\rangle\langle\alpha|d^2\alpha, \tag{3.1.1}$$

which according to Glauber is called as P representation [26]. $P(\alpha)$ that reflects the weight of coherent states in the above expansion, is titled as the Glauber-Sudarshan P function, for Sudarshan also observed the same form for the density operator [27]. This weight function can be considered similar to the probability density of different values of

α across the complex plane, if $P(\alpha) \geq 0$ or if it contains singularities as strong as delta function, which is so for coherent states.

Criteria for Nonclassicality

It turns out that for certain quantum states, $P(\alpha)$ ceases to be a Probability Distribution Function (PDF) owing to negative values in some part of phase space or has singularities stronger than delta function (i.e., derivative of delta function). The states for which $P(\alpha)$ can no longer be a true probability distribution function, are referred to as nonclassical and the corresponding P function qualifies as quasi-probability distribution.

Normalization of P Function

Just like any phase space probability distribution, the P function distribution when integrated across the entire complex plane gives 1. This can be asserted by using the definition of a mixed quantum state,

$$\hat{\rho} = \sum_i p_i |\psi_i\rangle\langle\psi_i|,$$

where, $|\psi_i\rangle$ represents a pure state, and p_i is the probability of finding the system in the ith pure state,

$$Tr(\hat{\rho}) = \sum_n \sum_i p_i \langle n|\psi_i\rangle\langle\psi_i|n\rangle,$$

with, $|n\rangle$ representing orthonormal basis, which forms a complete set i.e. $\sum_n |n\rangle\langle n| = 1$. Using completeness of $|n\rangle$ and normalizability of $|\psi_i\rangle$,

$$= \sum_i p_i,$$

$$= 1, \tag{3.1.2}$$

recalling Eq. (3.1.1) and Eq. (3.1.1), we get,

$$1 = Tr(\rho) = Tr \int P(\alpha)|\alpha\rangle\langle\alpha|d^2\alpha,$$

using property of trace,

$$= \int P(\alpha) \langle \alpha | \alpha \rangle d^2 \alpha,$$

$$= \int P(\alpha) d^2 \alpha.$$

Inadequacy of P Function in Phase Space Realization

A drawback of P function is that it constitutes tempered distribution, and is strictly speaking not a function. Unlike functions, the distributions represented by derivatives of delta function hold no meaning until they appear in an integral acting on a function, facilitating shift of derivative on to the function itself. Therefore, Wigner function discussed in the next paragraph is of primary interest for inferring nonclassicality of quantum states.

3.2 Nonclassicality Quantifiers

There are number of quantifiers of nonclassicality, with each having its own attributes, quantifying various aspects of nonclassicality. These include Wigner function, Mandel Q parameter, squeezing parameter, entanglement potential, measures of non-Gaussianity, resource and operational resource theory of nonclassicality [28] etc. Out of these we have discussed first two quantifiers in succeeding sections and the last one in next chapter.

3.2.1 Wigner Function

Another phase space quasi-probability distribution function which captures the nonclassical nature of states, called Wigner function, was first proposed by Wigner in 1932 and is defined as [41],

$$W(q,p) := \frac{1}{2\pi\hbar} \int_{-\infty}^{\infty} \langle q + \frac{1}{2}x | \hat{\rho} | q - \frac{1}{2}x \rangle e^{ipx/\hbar} dx, \tag{3.2.1}$$

and when integrated over entire phase space yields 1. For $\hat{\rho} = |\psi\rangle\langle\psi|$,

$$\int_{-\infty}^{\infty} W(q,p) dp dq = \frac{1}{2\pi\hbar} \left[\int_{-\infty}^{\infty} \psi^*(q + \frac{1}{2}x) \psi(q - \frac{1}{2}x) \left(\int_{-\infty}^{\infty} e^{ipx/\hbar} dp \right) dx dq \right],$$

28

using fourier transform of delta function,

$$= \int_{-\infty}^{\infty} |\psi(q)|^2 dq = 1.$$

Wigner function can be obtained as Fourier transform of a symmetric ordered characteristic function $C_s^{(\rho)}$ [42],

$$W(\alpha) = \frac{1}{\pi^2} \int e^{\lambda^* \alpha - \lambda \alpha^*} C_s^{(\rho)}(\lambda) d^2\lambda. \tag{3.2.2}$$

The characteristic functions of state of a system correspond to various orders in which $D(\lambda)$ is expanded in terms of creation and annihilation operator. Number operator $(\hat{a}^\dagger \hat{a})$ is in normal order, operator $\hat{a}\hat{a}^\dagger$ is ordered anti-normally, whereas, sum of these operators is symmetric. Thus, in general there are three characteristic functions given as under:

$$C_s^{(\rho)}(\lambda) = Tr[\hat{\rho}D(\lambda)] = Tr[\hat{\rho}e^{\lambda\hat{a}^\dagger - \lambda^*\hat{a}}], \tag{3.2.3}$$

$$C_n^{(\rho)}(\lambda) = Tr[\hat{\rho}e^{\lambda\hat{a}^\dagger} e^{-\lambda^*\hat{a}}], \tag{3.2.4}$$

$$C_{an}^{(\rho)}(\lambda) = Tr[\hat{\rho}e^{-\lambda^*\hat{a}} e^{\lambda\hat{a}^\dagger}], \tag{3.2.5}$$

where ρ is the density operator describing the state, $C_n^{(\rho)}(\lambda)$ and $C_{an}^{(\rho)}(\lambda)$ are the normal and anti-normal ordered characteristic functions, respectively. These functions are linked as,

$$C_s^{(\rho)}(\lambda) = C_n^{(\rho)}(\lambda)e^{-|\lambda|^2/2} = C_{an}^{(\rho)}(\lambda)e^{|\lambda|^2/2}, \tag{3.2.6}$$

and can be used to calculate Wigner functions of various states. We have worked out the Wigner functions of cats through normal ordered characteristic function as it reduces the complexity of the calculations.

3.2.2 Mandel Q Parameter

Mandel Q parameter helps in capturing the nonclassicality of states by quantifying the deviation of statistics of photon number of a particular optical field from that of classical

state. Mathematically, it is defined as [43],

$$Q := \frac{\langle (\Delta \hat{n})^2 \rangle - \langle \hat{n} \rangle}{\langle \hat{n} \rangle},$$

simplifying further,

$$
\begin{aligned}
&= \frac{\langle \hat{n}^2 \rangle - \langle \hat{n} \rangle^2 - \langle \hat{n} \rangle}{\langle \hat{n} \rangle}, \\
&= \frac{\langle \hat{a}^\dagger \hat{a} \hat{a}^\dagger \hat{a} \rangle - \langle \hat{a}^\dagger \hat{a} \rangle^2 - \langle \hat{a}^\dagger \hat{a} \rangle}{\langle \hat{a}^\dagger \hat{a} \rangle}, \\
&= \frac{\langle \hat{a}^\dagger \hat{a} \rangle + \langle \hat{a}^{\dagger 2} \hat{a}^2 \rangle - \langle \hat{a}^\dagger \hat{a} \rangle^2 - \langle \hat{a}^\dagger \hat{a} \rangle}{\langle \hat{a}^\dagger \hat{a} \rangle}, \\
&= \frac{\langle \hat{a}^{\dagger 2} \hat{a}^2 \rangle - \langle \hat{a}^\dagger \hat{a} \rangle^2}{\langle \hat{a}^\dagger \hat{a} \rangle},
\end{aligned}
\tag{3.2.7}
$$

where, $\langle (\Delta \hat{n})^2 \rangle$ is the variance in distribution of photon number. Q parameter help identify the nature of states as when :

Q = 0, indicates Poissonian character of states, which is typical of coherent states. Therefore, Poissonian behaviour is associated with classicality.

Q < 0, corresponds to sub-Poissonian statistics, which relates to non-classical state. This indicates less fluctuation in photon number than expected from classical states.

Q > 0, corresponds to super-Poissonian statistics which can hint towards classical (for thermal field) or non-classical light, making Q insufficient to assess the nature of state. For states showing such statistics, fluctuations in photon number is greater than the average photon number.
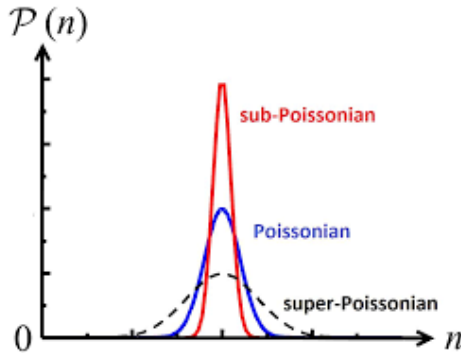
Figure 3.2.1: Types of Photon Number Distributions. Classical and nonclassical states follow Poissonian and sub-Poissonian statistics, respectively. Ambiguity prevails for nature of states showing super-Poissonian behaviour. [44]

3.3 Nature of Schrödinger Cat States

Equipped with the tools to investigate the nonclassicality of states, we now analyze the nature of multiheaded cats.

3.3.1 Wigner Function of Cats

The normal ordered characteristic function for even cat is:

$$C_{n(e)}(\lambda) = \langle \psi_e | e^{\lambda \hat{a}^\dagger} e^{-\lambda^* \hat{a}} | \psi_e \rangle,$$
$$= |N_e|^2 (\langle \alpha | + \langle -\alpha |) e^{\lambda \hat{a}^\dagger} e^{-\lambda^* \hat{a}} (|\alpha\rangle + |-\alpha\rangle),$$

using eq(2.1.16) and eq(A.1.1),

$$= |N_e|^2 [e^{\lambda \alpha^* - \lambda^* \alpha} + e^{-(\lambda \alpha^* - \lambda^* \alpha)} + e^{-2|\alpha|^2}(e^{\lambda \alpha^* + \lambda^* \alpha} + e^{-(\lambda \alpha^* + \lambda^* \alpha)})], \qquad (3.3.1)$$
$$= \frac{2|N_e|^2}{\pi} \left[e^{-2|\beta - \alpha|^2} + e^{-2|\beta + \alpha|^2} + 2e^{-2|\beta|^2} \cos 2i(\alpha \beta^* - \alpha^* \beta) \right],$$

The Wigner function becomes,

$$W_e(\beta) = \frac{2|N_e|^2}{\pi} \left[e^{-2|\beta - \alpha|^2} + e^{-2|\beta + \alpha|^2} + 2e^{-2|\beta|^2} \cos 4\mathrm{Im}(\alpha \beta^*) \right],$$

which for real α reduce to,

$$W_e(\beta) = \frac{2|N_e|^2}{\pi} \left[e^{-2[(\beta_r - \alpha_r)^2 + \beta_i^2]} + e^{-2[(\beta_r + \alpha_r)^2 + \beta_i^2]} + 2e^{-2(\beta_r^2 + \beta_i^2)} \cos 4(\alpha_r \beta_i) \right]. \qquad (3.3.2)$$
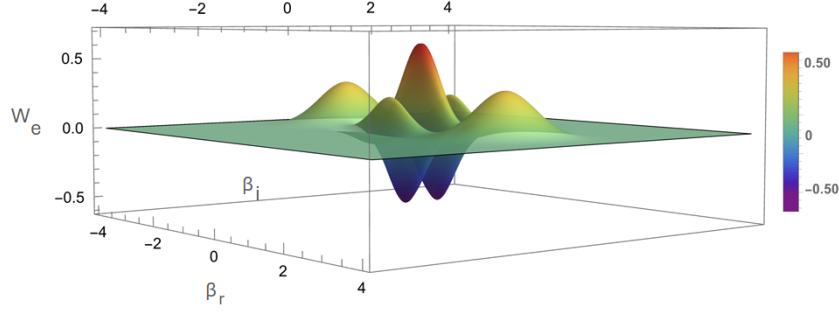
(a) Plot of W_e Vs β
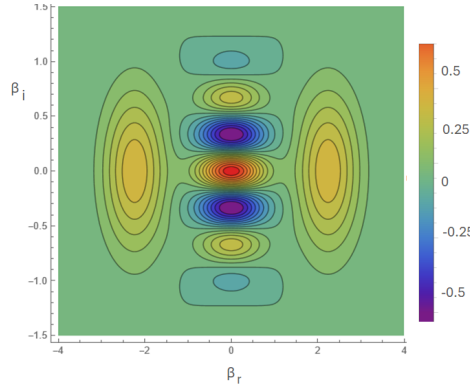
(b) Projection of W_e

Figure 3.3.1: Wigner Function of even cat for $\alpha = \sqrt{5}$. (a) Gaussian curves reflect the alive and dead components of the Schrödinger cat at $\alpha = \pm\sqrt{5}$, with interference fringes between them. The negative curves in the fringe pattern indicate nonclassicality of even cat.

Key Features of Wigner Function of Even Cats

Wigner plot of even cats, has certain prominent and peculiar features, such as,

Gaussian Curves   The first two terms of the Wigner function represent two Gaussian curves which are obtained due to overlap of each coherent state with itself. $e^{-2|\beta-\alpha|^2}$ appears due to $|\alpha\rangle$ and peaks at $\beta = \alpha$ i.e. $\beta_r = \sqrt{5}$ and $\beta_i = 0$ as we have plotted the function for real α. The second Gaussian term is again due to $|-\alpha\rangle$ with maximum at $\beta_r = -\sqrt{5}$ and $\beta_i = 0$.

Interference Fringes The fringes in the centre are due to interference between the two coherent states, reflecting coherence terms and superposition. The oscillations in the fringes is due to the cosine function in the last term $e^{-2|\beta|^2}\cos 2\text{Im}(\alpha\beta^*)$; whereas the Gaussian function centered at zero modulates the oscillations ensuring that the amplitude dies down as β increases. The valleys in the interference pattern, where Wigner function becomes negative, are indicative of nonclassicality of even cat.

Similarly, Wigner functions for odd cat is:

$$W_o(\beta) = \frac{2|N_o|^2}{\pi} \left[e^{-2|\beta-\alpha|^2} + e^{-2|\beta+\alpha|^2} - 2e^{-2|\beta|^2} \cos 4\mathrm{Im}(\alpha\beta^*) \right],$$

for real α,

$$= \frac{2|N_o|^2}{\pi} \left[e^{-2[(\beta_r-\alpha_r)^2+\beta_i^2]} + e^{-2[(\beta_r+\alpha_r)^2+\beta_i^2]} - 2e^{-2(\beta_r^2+\beta_i^2)} \cos 4(\alpha_r\beta_i) \right]. \quad (3.3.3)$$
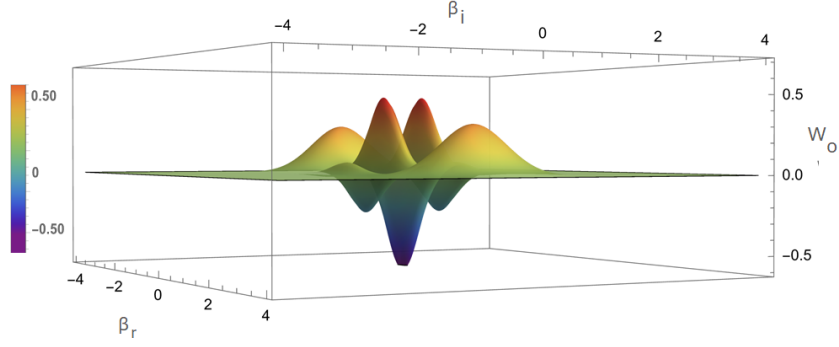
(a) Plot of W_o Vs β
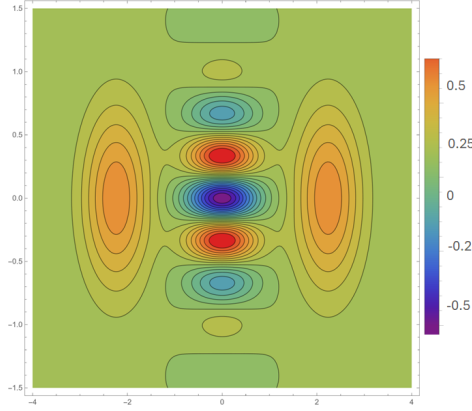
(b) Projection of W_o

Figure 3.3.2: Wigner Function of odd cat with $\alpha = \sqrt{5}$. (a) Gaussian curves are same as for even cat at $\alpha = \pm\sqrt{5}$. The fringe pattern again has negative values indicating nonclassicality of odd cats; however, due to inversion of fringes the negativity of Wigner function of even and odd cats will differ.

The Wigner function of odd cats share similar key features as that of even cats, i.e. with two Gaussian curves peaked at $(\beta_r, \beta_i) = (\pm\sqrt{5}, 0)$ and an interference pattern. However, the defining feature of odd cats is its inverted fringe pattern, which contains a central negative peak with alternating adjacent peaks. Thus, odd cat is also nonclassical

due to negativity of its Wigner function.

For YS state, due to presence of additional phase difference in coherent states, the Wigner function changes to,

$$W_{ys}(\beta) = \frac{1}{\pi}\left[e^{-2|\beta-\alpha|^2} + e^{-2|\beta+\alpha|^2} + 2e^{-2|\beta|^2}\sin 4\text{Im}(\alpha\beta^*)\right],$$

for real α,

$$= \frac{1}{\pi}\left[e^{-2[(\beta_r-\alpha_r)^2+\beta_i^2]} + e^{-2[(\beta_r+\alpha_r)^2+\beta_i^2]} - 2e^{-2(\beta_r^2+\beta_i^2)}\sin 4(\alpha_r\beta_i)\right]. \qquad (3.3.4)$$
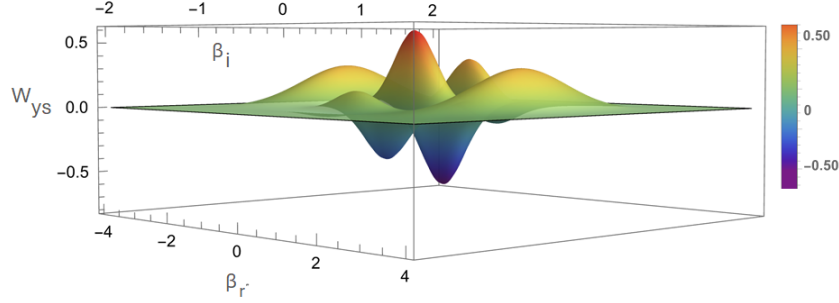
(a) Plot of W_{ys} Vs β
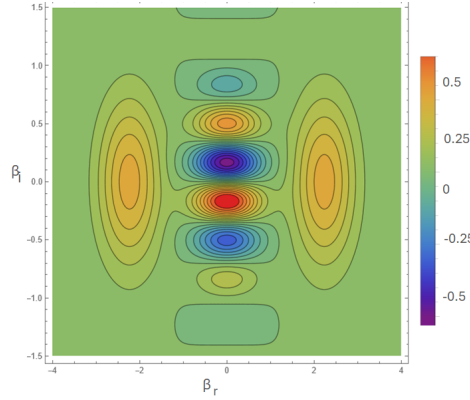
(b) Projection of W_{ys}

Figure 3.3.3: Wigner Function of YS state with $\alpha = \sqrt{5}$. Apart from Gaussian curves which share same properties with even and odd cats, the interference pattern shows oscillations which are signature of sine function. Negative curves of the fringes hint towards nonclassicality of the states.

Once again, the Wigner function for YS state only differ in its fringe pattern, which shows oscillatory behaviour depicted by sine function and modulated by Gaussian. Due to sine function, which is out of phase by 90° to the cosine function in even and odd cats,

additional phase shift is introduced and the negative central peak of Gaussian envelope is shifted at $\beta_i = \pi/2k$ where $k = 4\alpha_r$. The negative values of Wigner function of YS cat is indicative of nonclassicality.

For 3H and 4H, the plots for Wigner functions are:
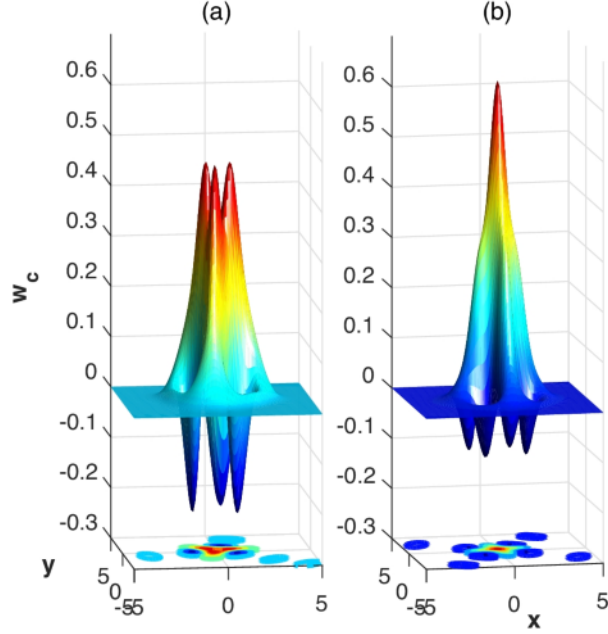
Figure 3.3.4: Wigner Functions for 3H and 4H [32]

From Fig. 3.3.4 it is evident that the Wigner function of these cats assume negative values in phase space. The interference pattern differs substantially from that of cats and YS state. Apart from the general features, the negativity of Wigner function reflects that 3 and 4H cats are nonclassical as well.

3.3.2 Q Parameter for Cats

Recalling eq. (3.2.7), in this section we have calculated the Q parameter of multiheaded cats and their excited counterparts, and then Q parameter for cats have been plotted for analysis of their photon statistics.

Even Cats

For even cats given by eq. (2.2.1), evaluating the averages involved in definition of Q:

$$\langle \psi_e | \hat{a}^\dagger \hat{a} | \psi_e \rangle = N_e^2 (\langle \alpha | + \langle -\alpha |) \hat{a}^\dagger \hat{a} (|\alpha\rangle + |-\alpha\rangle),$$

using Eq. (A.1.1), $\langle \pm \alpha | \mp \alpha \rangle = e^{-2|\alpha|^2}$,

$$= |\alpha|^2 N_e^2 / N_o^2. \tag{3.3.5}$$

As 2H cats are eigenstate of $\hat{a}^2$,

$$\langle \psi_e | \hat{a}^{\dagger 2} \hat{a}^2 | \psi_e \rangle = |\alpha|^4. \tag{3.3.6}$$

Hence, Eq. (3.2.7) becomes,

$$
\begin{aligned}
Q_e &= \frac{|\alpha|^2 (N_o^4 - N_e^4)}{N_e^2 N_o^2}, \\
&= \frac{4|\alpha|^2 e^{-2|\alpha|^2}}{1 - e^{-4|\alpha|^2}} > 0.
\end{aligned}
\tag{3.3.7}
$$

Thus, even cats follow super-Poissonian statistics and their nonclassicality cannot be concluded from Q alone.

Odd Cats

Recalling odd cats given by eq. (2.2.2),

$$\langle \psi_o | \hat{a}^\dagger \hat{a} | \psi_o \rangle = |\alpha|^2 N_o^2 / N_e^2. \tag{3.3.8}$$

Q parameter for odd cat, Q_o, is given as,

$$
\begin{aligned}
Q_o &= \frac{|\alpha|^2 (N_e^4 - N_o^4)}{N_e^2 N_o^2}, \\
&= -\frac{4|\alpha|^2 e^{-2|\alpha|^2}}{1 - e^{-4|\alpha|^2}} < 0,
\end{aligned}
\tag{3.3.9}
$$

which hint towards sub-Poissonian statistics, capturing nonclassicality of these cats.

YS States

For YS states, as given in eq. (2.2.4), evaluating the averages involved in Q,

$$\langle\psi_{ys}|\hat{a}^\dagger\hat{a}|\psi_{ys}\rangle = \frac{1}{2}((\langle\alpha| - i\langle-\alpha|)\hat{a}^\dagger\hat{a}(|\alpha\rangle + i|-\alpha\rangle)),$$
$$= |\alpha|^2. \tag{3.3.10}$$

The corresponding Q parameter Q_{ys} becomes,

$$Q_{ys} = \frac{|\alpha|^4 - |\alpha|^4}{|\alpha|^2},$$
$$= 0, \tag{3.3.11}$$

which represent YS states as classical owing to their Poissonian photon statistics.

3H Cats

Evaluating the averages involved in Mandel Q for 3H cats,

$$\langle\psi_{3h}|\hat{a}^\dagger\hat{a}|\psi_{3h}\rangle = 2N_{3h}^2|\alpha|^2(1 - e^{-2|\alpha|^2}),$$
$$= \frac{N_{3h}^2|\alpha|^2}{N_o^2}. \tag{3.3.12}$$
$$\langle\psi_{3h}|\hat{a}^{\dagger2}\hat{a}^2|\psi_{3h}\rangle = \frac{N_{3h}^2|\alpha|^4}{N_e^2}. \tag{3.3.13}$$

Mandel Q parameter for 3H cats Q_{3h} becomes,

$$Q_{3h} = \frac{N_{3h}^2|\alpha|^4/N_e^2 - N_{3h}^4|\alpha|^4/N_o^4}{N_{3h}^2|\alpha|^2/N_o^2},$$
$$= |\alpha|^2\left(\frac{N_o^2}{N_e^2} - \frac{N_{3h}^2}{N_o^2}\right) > 0, \tag{3.3.14}$$

reflecting super-Poissonian characteristics.

4H Cats

Evaluating the averages involved in Mandel Q,

$$\langle\psi_{4h}|\hat{a}^\dagger\hat{a}|\psi_{4h}\rangle = \frac{1}{4}((\langle\alpha| - \langle i\alpha| + \langle-\alpha| + \langle-i\alpha|)\hat{a}^\dagger\hat{a}(|\alpha\rangle - |i\alpha\rangle + |-\alpha\rangle + |-i\alpha\rangle)),$$

using Eq. (A.1.1), $\langle \pm\alpha| \pm i\alpha\rangle = \langle \pm i\alpha| \mp \alpha\rangle = e^{-|\alpha|^2}e^{i|\alpha|^2}$, $\langle \pm\alpha| \mp i\alpha\rangle = \langle \pm i\alpha| \pm \alpha\rangle = e^{-|\alpha|^2}e^{-i|\alpha|^2}$ and $\langle \pm i\alpha| \mp i\alpha\rangle = e^{-2|\alpha|^2}$,

$$= |\alpha|^2. \tag{3.3.15}$$

$$\langle\psi_{4h}|\hat{a}^{\dagger 2}\hat{a}^2|\psi_{4h}\rangle = |\alpha|^4. \tag{3.3.16}$$

Q_{4h} becomes,

$$Q_{4h} = \frac{|\alpha|^4 - |\alpha|^4}{|\alpha|^2},$$

$$= 0. \tag{3.3.17}$$

Hence, 4H cats like YS display classical character according to Q parameter.

Excited Even Cat

Evaluating the averages involved in Q for excited even cats,

$$\langle\psi_{eec}|\hat{a}^{\dagger}\hat{a}|\psi_{eec}\rangle = N_{eec}^2\langle\psi_e|\hat{a}\hat{a}^{\dagger}\hat{a}\hat{a}^{\dagger}|\psi_e\rangle,$$

using commutator $[\hat{a}, \hat{a}^{\dagger}] = 1$,

$$= N_{eec}^2\langle\psi_e|1 + 3\hat{a}^{\dagger}\hat{a} + \hat{a}^{\dagger 2}\hat{a}^2|\psi_e\rangle.$$

Recalling results obtained for even cats,

$$= N_{eec}^2(1 + 3|\alpha|^2\frac{N_e^2}{N_o^2} + |\alpha|^4). \tag{3.3.18}$$

$$\langle\psi_{eec}|\hat{a}^{\dagger 2}\hat{a}^2|\psi_{eec}\rangle = N_{eec}^2\langle\psi_e|\hat{a}\hat{a}^{\dagger 2}\hat{a}^2\hat{a}^{\dagger}|\psi_e\rangle,$$

$$= N_{eec}^2\langle\psi_e|4\hat{a}^{\dagger}\hat{a} + 5\hat{a}^{\dagger 2}\hat{a}^2 + \hat{a}^{\dagger 3}\hat{a}^3|\psi_e\rangle,$$

$$= N_{eec}^2\left[4|\alpha|^2\frac{N_e^2}{N_o^2} + 5|\alpha|^4 + |\alpha|^6\frac{N_e^2}{N_o^2}\right]. \tag{3.3.19}$$

Mandel Q for excited even cat Q_{eec} becomes,

$$Q_{eec} = \frac{N_{eec}^2 \left[4|\alpha|^2 \frac{N_e^2}{N_o^2} + 5|\alpha|^4 + |\alpha|^6 \frac{N_e^2}{N_o^2}\right] - N_{eec}^4 (1 + 3|\alpha|^2 \frac{N_e^2}{N_o^2} + |\alpha|^4)^2}{N_{eec}^2 (1 + 3|\alpha|^2 \frac{N_e^2}{N_o^2} + |\alpha|^4)},$$

$$= -\frac{16|\alpha|^8 N_o^4 N_e^4 e^{-2|\alpha|^2} + 8|\alpha|^4 (1 + e^{-4|\alpha|^2} - 8e^{-2|\alpha|^2}) N_o^4 N_e^4 + N_o^4 + 2|\alpha|^2 N_o^2 N_e^2}{(N_o^2 + |\alpha|^2 N_e^2)(3|\alpha|^2 N_e^2 + N_o^2 + |\alpha|^4 N_o^2)} < 0.$$

$$(3.3.20)$$

Thus, even though even cat displayed super-Poissonian statistics; its excited counterpart clearly follows sub-Poisson statistics.

Excited Odd Cats

Evaluating the averages involved in Q,

$$\langle \psi_{eoc} | \hat{a}^\dagger \hat{a} | \psi_{eoc} \rangle = N_{eoc}^2 (1 + 3|\alpha|^2 \frac{N_o^2}{N_e^2} + |\alpha|^4). \tag{3.3.21}$$

$$\langle \psi_{eoc} | \hat{a}^{\dagger 2} \hat{a}^2 | \psi_{eoc} \rangle = N_{eoc}^2 \langle \psi_o | 4\hat{a}^\dagger \hat{a} + 5\hat{a}^{\dagger 2} \hat{a}^2 + \hat{a}^{\dagger 3} \hat{a}^3 | \psi_o \rangle,$$

$$= N_{eoc}^2 \left[4|\alpha|^2 \frac{N_o^2}{N_e^2} + 5|\alpha|^4 + |\alpha|^6 \frac{N_o^2}{N_e^2}\right]. \tag{3.3.22}$$

Q_{eoc} becomes,

$$Q_{eoc} = \frac{N_{eoc}^2 \left[4|\alpha|^2 \frac{N_o^2}{N_e^2} + 5|\alpha|^4 + |\alpha|^6 \frac{N_o^2}{N_e^2}\right] - N_{eoc}^4 (1 + 3|\alpha|^2 \frac{N_o^2}{N_e^2} + |\alpha|^4)^2}{N_{eoc}^2 (1 + 3|\alpha|^2 \frac{N_o^2}{N_e^2} + |\alpha|^4)},$$

$$= \frac{16|\alpha|^8 N_o^4 N_e^4 e^{-2|\alpha|^2} - 8|\alpha|^4 (1 + e^{-4|\alpha|^2} + 8e^{-2|\alpha|^2}) N_o^4 N_e^4 - N_e^4 - 2|\alpha|^2 N_o^2 N_e^2}{(N_e^2 + |\alpha|^2 N_o^2)(3|\alpha|^2 N_o^2 + N_e^2 + |\alpha|^4 N_e^2)}.$$

$$(3.3.23)$$

By plotting the above result, we learn that $Q_{eoc} < 0$; hence, excited odd cat follow sub-Poissonian statistics.

Excited YS States

Evaluating the averages involved in Q,

$$\langle \psi_{eys} | \hat{a}^\dagger \hat{a} | \psi_{eys} \rangle = N_{eys}^2 (1 + 3|\alpha|^2 + |\alpha|^4). \tag{3.3.24}$$

$$\langle \psi_{eys} | \hat{a}^{\dagger 2} \hat{a}^2 | \psi_{eys} \rangle = N_{eys}^2 \left[4|\alpha|^2 + 5|\alpha|^4 + |\alpha|^6\right]. \tag{3.3.25}$$

Q_{eys} becomes,

$$Q_{eys} = -N_{eys}^2 \frac{1 + 2|\alpha|^2 + 2|\alpha|^4}{1 + 3|\alpha|^2 + |\alpha|^4} < 0. \tag{3.3.26}$$

Hence, nonclassicality of excited YS state is captured by Q parameter as opposed to their non-excited counterparts, for which Q_{ys} was 0.

Excited 3H Cats

Evaluating the averages involved in Q,

$$\langle\psi_{e3h}|\hat{a}^\dagger\hat{a}|\psi_{e3h}\rangle = N_{e3h}^2(1 + 3|\alpha|^2\frac{N_{3h}^2}{N_o^2}N_o^2 + |\alpha|^4\frac{N_{3h}^2}{N_e^2}).$$

$$\langle\psi_{e3h}|\hat{a}^{\dagger 2}\hat{a}^2|\psi_{e3h}\rangle = N_{e3h}^2\Big[4|\alpha|^2\frac{N_{3h}^2}{N_o^2} + 5|\alpha|^4\frac{N_{3h}^2}{N_e^2} + |\alpha|^6\frac{N_{3h}^2}{N_o^2}\Big]. \tag{3.3.27}$$

Q_{e3h} becomes,

$$Q_{e3h} = \Big[N_{e3h}^2|\alpha|^2 N_{3h}^4\big[-12 - 2|\alpha|^2 + 2|\alpha|^4 + e^{-|\alpha|^2/2}(24|\alpha|^2 - 16 + 8|\alpha|^4)$$

$$+e^{-2|\alpha|^2}(4 + 70|\alpha|^2 - 2|\alpha|^4 - 16|\alpha|^6) + e^{-5|\alpha|^2/2}(24|\alpha|^2 + 16 - 8|\alpha|^4)$$

$$+e^{-4|\alpha|^2}(8 - 8|\alpha|^2)\big] - N_{e3h}^2\Big] \Big/ \big(1 + 3|\alpha|^2\frac{N_{3h}^2}{N_o^2} + |\alpha|^4\frac{N_{3h}^2}{N_e^2}\big). \tag{3.3.28}$$

Plotting the above result shows that $Q_{e3h} < 0$, as opposed to positive values of Q for 3H state.

Excited 4H Cats

Evaluating the averages involved in Q,

$$\langle\psi_{e4h}|\hat{a}^\dagger\hat{a}|\psi_{e4h}\rangle = N_{e4h}^2\big(1 + 3|\alpha|^2 + |\alpha|^4\big). \tag{3.3.29}$$

$$\langle\psi_{e4h}|\hat{a}^{\dagger 2}\hat{a}^2|\psi_{e4h}\rangle = N_{e4h}^2\big(4|\alpha|^2 + 5|\alpha|^4 + |\alpha|^6\big). \tag{3.3.30}$$

Q_{e4h} becomes,

$$Q_{e4h} = -\frac{2|\alpha|^2}{1 + 3|\alpha|^2 + |\alpha|^4} < 0. \tag{3.3.31}$$

As opposed to 4H cats for which $Q = 0$, for excited 4H cat Q attains negative values reflecting nonclassical attribute.

Fig. 3.3.5 reflect that among Schrödiner cats Q parameter is negative for odd cats only; thus qualifying it as noncalssical state. YS state is tagged as classical state, owing to zero value of Q which is not in consonance with negativity of corresponding Wigner function. Hence, Q is unable to capture any nonclassical aspect of this state. For even cat, Q being greater than zero reveals super-Poissonian statistics. In such instances, ambiguity prevails in interpreting the nature of state as super-Poissonian character can be inferred either as classical or nonclassical. Similarly, Q identifies 4H cat as classical for $Q_{4h} = 0$ and fails to distinguish 3H cat as classical or nonclassical as $Q_{3h} > 0$.
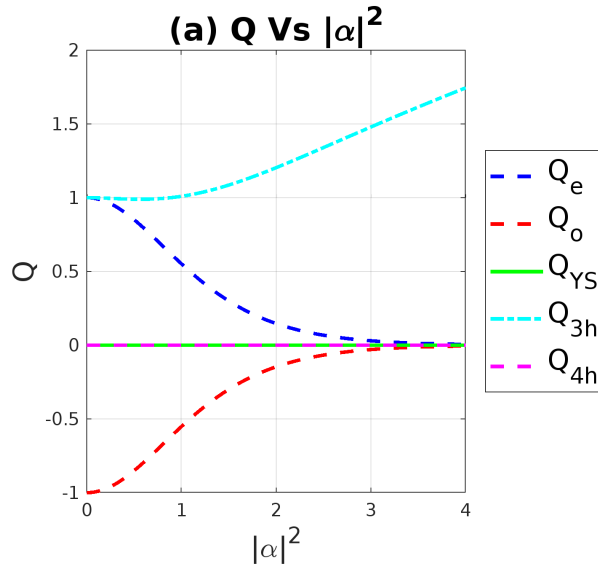
Figure 3.3.5: Plot of Q parameter vs $|\alpha|^2$ for cats. Q only qualifies odd cat as nonclassical, and shows ambiguity in inferring nonclassicality

Even though Q parameter is not capturing the nonclassicality of the cats in entirety, it may hold some bearing over metrological ability of the states. It is this aspect that we intend to explore.

Chapter 4

Operational Quantification of Nonclassicality via Quantum Metrology

In this chapter, we have first explored various quantum tasks involved in quantum metrology for undergoing parameter estimation, followed by detail review of classical versus quantum estimation theory. In the end, we have discussed the operational quantifiers of nonclassicality that define nonclassicality in terms of any advantage that they offer in carrying out a quantum task.

4.1 Quantum Metrology

Quantum metrology has already been introduced in Chapter 1 along with cursory mention of steps involved in it, here we discuss its various quantum mechanical aspects, in detail.

4.1.1 Estimation Tasks in Quantum Metrology

The most significant part of the quantum metrology is the selection of a nonclassical state $\hat{\rho}$, called as probe, that optimizes the parameter estimation. It will be shown in chapter 6 that probe optimized for estimation of one parameter may not necessarily be optimized for another parameter. The unknown parameter ϕ, which is to be estimated by the process, is encoded onto the probe state through unitary quantum mapping, which gives rise to a state that now depends on ϕ as $\hat{\rho}_\phi = e^{-i\phi\hat{G}}\hat{\rho}e^{i\phi\hat{G}}$ where, $\hat{G}$ is the

generator of the transformation caused by quantum mapping. Performing estimation of the parameter requires that a measurement be performed on $\hat{\rho}_\phi$, which in quantum metrology is represented by generalized measurements called as Positive Operator Valued Measurements (POVM) [45]. $\{\hat{\Pi}_\mu\}$ represent hermitian elements of POVM and satisfy certain relations, such as decomposition of unity $\int \hat{\Pi}_\mu \, d\mu = 1$ and $\hat{\Pi}_\mu \geq 0$. Projection operators are special type of these generalized measurements. Once the measurement is performed, the readouts satisfy the PDF $p(\mu|\phi) = Tr(\hat{\Pi}_\mu \hat{\rho}_\phi)$. Now the problem at hand has reduced to that of classical parameter estimation. However, selection of a particular POVM from infinite options will impact the parameter estimation and thus needs optimization as well.
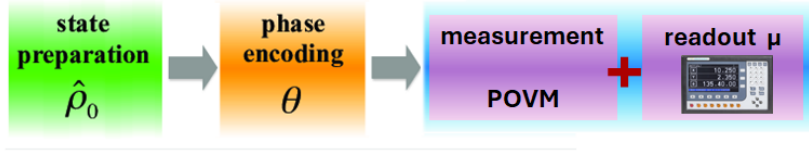
Figure 4.1.1: Steps in Quantum Metrology

4.1.2   Classical Parameter Estimation

The problem of classical estimation theory tantamount to finding an unbiased estimator Φ that maps the results $\{\mu\}$ of measurements of a system, to an unknown parameter $\{\phi\}$ [46]. The measurement outcomes μ follow a certain PDF $p(\mu|\phi)$ and follow normalization condition, $\int p(\mu|\phi)d\mu = 1$. Our guess of unknown parameter can be correct if we repeat the experiment multiple times, which translates to the accuracy of the estimator deeming it unbiased, i.e.,

$$\langle \Phi \rangle = \int p(\mu|\phi)\Phi d\mu(\mu) = \phi. \tag{4.1.1}$$

Here, ϕ represents the true value of unknown parameter. In order to look for an efficient estimator we need to define a quantity called Fisher Information (FI). FI is defined as the average of square of derivative of log likelihood function taken over entire values of

outcomes μ,

$$F(\phi) := \left\langle \left[\partial_\phi \log p(\mu|\phi) \right]^2 \right\rangle, \tag{4.1.2}$$

$$= \int d\mu \big(\partial_\phi \log p(\mu|\phi) \big)^2,$$

$$= \int d\mu \frac{1}{p(\mu|\phi)} \left(\partial_\phi p(\mu|\phi) \right)^2, \tag{4.1.3}$$

which in terms of log likelihood $L(\mu|\phi) = \log p(\mu|\phi)$ can be written as,

$$= \left\langle \left[\partial_\phi L(\mu|\phi) \right]^2 \right\rangle, \tag{4.1.4}$$

where Likelihood function finds the best PDF that fits the given data i.e., measurement outcomes, for a given value of ϕ. The efficiency with which an estimator estimates the unknown parameter is given by Cramer-Rao Bound (CRB) (appendix C.1),

$$\Delta^2 \hat{\Phi} \geq \frac{1}{NF(\phi)}, \tag{4.1.5}$$

where N is the number of times measurement is performed. The estimators saturating the CRB are termed as the most efficient.

4.1.3 Quantum Estimation Theory

Transition from classical to quantum estimation theory calls for considering quantum states for probes and POVM for carrying out measurements. Addressing the optimal selection of POVM for quantum metrology mandates introduction of a hermitian operator called as Symmetric Logarithmic Derivative (SLD)[28]. This operator satisfies following equation,

$$\partial_\phi \hat{\rho}_\phi = \frac{1}{2} \{ \hat{\rho}_\phi, \hat{L}_\phi \}, \tag{4.1.6}$$

with $\hat{\rho}_\phi$ to be taken as a mixed state i.e., $\hat{\rho}_\phi = \sum_k p_k |\psi_k\rangle\langle\psi_k|$, $\hat{L}_\phi$ turns out as under (appendix C.2),

$$\hat{L}_\phi = 2 \sum_{k,l} \frac{(\partial_\phi \hat{\rho}_\phi)_{kl} |\psi_k\rangle\langle\psi_l|}{p_k + p_l}, \tag{4.1.7}$$

Using eq. (4.1.6) together with eq. (4.1.7) leads to,

$$F(\phi) \leq Tr[\hat{\rho}_\phi \hat{L}_\phi^2],$$

where, the RHS of the inequality is defined as Quantum Fisher Information (QFI)

$$F_Q(\hat{\rho}, \phi) := Tr[\hat{\rho}_\phi \hat{L}_\phi^2] \quad [46], \tag{4.1.8}$$

from which quantum CRB follows as,

$$\Delta^2 \hat{\Phi} \geq \frac{1}{N F_Q(\hat{\rho}, \phi)}. \tag{4.1.9}$$

Dependence of QFI on probe state as well as parameter ϕ reflects that the usefulness of the probe state alone for metrology is compromised. The problem can however be remedied by use of unitary transformation of the probe i.e., when $\hat{\rho}_\phi = e^{-i\phi\hat{G}}\hat{\rho}e^{i\phi\hat{G}}$, where $\hat{U} = e^{-i\phi\hat{G}}$ is the unitary operator that evolves the probe. Using definition of QFI eq. (4.1.8), eq. (4.1.7) and $\partial_\phi \hat{\rho}_\phi = i[\hat{\rho}_\phi, \hat{G}]$, we are led to following expression for QFI (appendix C.4),

$$F_Q(\hat{\rho}, \hat{G}) = 2 \sum_{kl} \frac{(p_k - p_l)^2}{p_k + p_l} |\hat{G}_{kl}|^2, \tag{4.1.10}$$

which now is independent of the unknown parameter. For pure $\hat{\rho} = |\psi\rangle\langle\psi|$ and mixed state $\hat{\rho} = \sum p_k |\psi_k\rangle\langle\psi_k|$, the above equation reduces to (appendix C.5),

$$F_Q(|\psi\rangle, \hat{G}) = 4\langle\psi|(\Delta\hat{G})^2|\psi\rangle, \tag{4.1.11}$$

$$F_Q(\hat{\rho}, \hat{G}) \leq 4Tr[\hat{\rho}(\Delta\hat{G})^2], \tag{4.1.12}$$

respectively.

Thus, QFI for pure and mixed states with respect to different parameters i.e., quadrature and phase sensing are defined as under (dropping the factor of 4 for convenience),

Pure States

QFI for quadrature and phase measurement are given as:

$$F_{\hat{X}}(|\psi\rangle) = \max_{\mu}\langle\psi|(\Delta\hat{X}_{\mu})^2|\psi\rangle, \tag{4.1.13}$$

where, $\hat{X}_{\mu} = i(e^{-i\mu}\hat{a}^{\dagger} - e^{i\mu}\hat{a})/\sqrt{2}$ and $\mu \in [0, 2\pi]$, which gives quadrature operators as $\hat{X}_{\pi/2} = (\hat{a}^{\dagger} + \hat{a})/\sqrt{2}$ and $\hat{X}_0 = (\hat{a} - \hat{a}^{\dagger})/\sqrt{2}i$.

$$F_{\hat{n}}(|\psi\rangle) = \langle\psi|(\Delta\hat{n})^2|\psi\rangle. \tag{4.1.14}$$

Mixed States

QFI for mixed states is defines as convex roof of variance [47],

$$F_{\hat{X}}(\hat{\rho}) = \max_{\mu}\left\{\min_{\{p_j, |\psi_j\rangle\}}\left(\sum p_j\langle\psi_j|(\Delta\hat{X}_{\mu})^2|\psi_j\rangle\right)\right\} [23], \tag{4.1.15}$$

$$F_{\hat{n}}(\hat{\rho}) = \left\{\min_{\{p_j, |\psi_j\rangle\}}\left(\sum p_j\langle\psi_j|(\Delta\hat{n})^2|\psi_j\rangle\right)\right\}, \tag{4.1.16}$$

with minimization over all ensembles.

Taking QFI as the measurement scheme, various probe states can be used to find as to which states offer optimal precision.

4.2   Operational Quantifiers of Nonclassicality

Nonclassicality of a state can be exploited to enhance the performance of a probe in metrology. The parameters that quantify the ability of a nonclassical state to enhance any quantum metrological task can be called as operational quantifiers. In following subsections, we have discussed two such quantifiers, one being metrological power of a state and the other as operational resource measure. The later gives a tight upper bound on the metrological power for displacement sensing.

4.2.1 Metrological Power of Nonclassical States

Metrological power of a probe is defined by the amount its QFI exceeds relative to that of any classical state, i.e.,

$$W_{\hat{G}}(\hat{\rho}) := \max[F_{\hat{G}}(\hat{\rho}) - F_{\hat{G}}(\hat{\rho}_{cl}), 0]. \tag{4.2.1}$$

Note that we have dropped the subscript Q from QFI as in earlier notation $F_Q(\hat{\rho}, \hat{G})$ and labelled it as $F_{\hat{G}}(\hat{\rho})$ as it is understood to be quantum Fisher information.

Quadrature Sensing

The metrological power of a state for quadrature sensing can be inferred from eq. (4.2.5) and is given as [23],

$$W_{\hat{X}}(\hat{\rho}) = \max[F_{\hat{X}}(\hat{\rho}) - F_{\hat{X}}(\hat{\rho}_{cl}), 0], \tag{4.2.2}$$

since metrological power of a probe is defined by taking classical state as benchmark, any negative outcome holds no significance. In that case, the quantity may very well be equated to zero. $F_{\hat{X}}(\hat{\rho}_{cl})$ for coherent state via eq. (4.1.13) becomes,

$$
\begin{aligned}
F_{\hat{X}}(\hat{\rho}_{cl}) &= \max_{\mu} \left\{ \langle \alpha | \hat{X}^2 | \alpha \rangle - \langle \alpha | \hat{X} | \alpha \rangle^2 \right\}, \\
&= \max_{\mu} \left\{ \frac{-1}{2}(e^{-2i\mu}\alpha^{*2} + e^{2i\mu}\alpha^2 - 2|\alpha|^2 - 1) + \frac{1}{2}(e^{-i\mu}\alpha^* - e^{i\mu}\alpha)^2 \right\},
\end{aligned}
$$

maximizing over μ yields,

$$
\begin{aligned}
&= |\alpha|^2 + \frac{1}{2} - |\alpha|^2, \\
&= \frac{1}{2}, \tag{4.2.3}
\end{aligned}
$$

hence, metrological power of any state is,

$$W_{\hat{X}}(\hat{\rho}) = \max[F_{\hat{X}}(\hat{\rho}) - 1/2, 0]. \tag{4.2.4}$$

Phase Sensing

For phase sensing, eq. (4.2.5) becomes,

$$W_{\hat{n}}(\hat{\rho}) = \max[F_{\hat{n}}(\hat{\rho}) - |\alpha|^2, 0], \tag{4.2.5}$$

as, $F_{\hat{n}}(\hat{\rho}_{cl}) = \langle \alpha | (\Delta \hat{n})^2 | \alpha \rangle = |\alpha|^2$.

Metrological power of a state can be considered as a criterion for nonclassicality. It is pertinent to mention here that metrological power does not quantify nonclassicality but its ability to enhance metrology. Here comes the notion of useful nonclassicality. Entirety of nonclassicality cannot be converted into useful quantum task; only useful nonclassicality can. We will see for cats, that although all are characterized as nonclassical states (evident from their Wigner functions), only few offer metrological advantage

4.2.2 Operational Resource Theory of Nonclassicality

Resource Theory of Nonclassicality

Resource Theories (RT) offer yet another way of quantifying the nonclassicality of states. There exist a number of RTs e.g., RT of entanglement, non-Gaussianity and nonclassicality which share same underlying approach. The objective of these theories is to identify the various attributes of nonclassicality of states which are otherwise not available freely i.e., via classical or free operations. Under Resource theoretic formalism, the nonclassical quantum states are considered as a resource, which provide means to counter the limits associated with classical states. A classical operation is defined as a quantum map which cannot produce nonclassicality from classical states. For RT of nonclassicality, free operations forbid creation of quantum resource such as superposition of classical states from their mixture. These operations can be of following forms:

- enhancing the number of classical states in a system, e.g., making a mixture of coherent states,

- applying passive optical operations that are linear, and

- removing the ancillary modes via trace.

A nonclassicality measure, $N(\hat{\rho})$, of resource theory must satisfy following conditions [28]:

- **Non-negativity i.e.** $N(\hat{\rho}) \geq 0$

  Equality holds if and only if the state is classical. This means that if the state being analyzed is nonclassical then the measure will be greater than zero, thus quantifying some aspect of quantumness of the state.

- **Weak Monotonicity i.e.** $N(\wedge[\hat{\rho}]) \leq N(\hat{\rho})$

  The statement entails monotonic decrease of $N(\hat{\rho})$ under operations represented by $\wedge$, where $\wedge$ represents linear maps. This condition is signature of all RTs. It forbids the creation and enhancement of nonclassicality freely, which signifies that it is impossible for the measure to increase under any linear operation.

- **Convexity i.e.** $\sum_j p_j N(\hat{\rho}_j) \geq N(\sum_j p_j \hat{\rho}_j)$

  Forming a mixture of states is a classical operation. This condition ensures that for a mixture of states, either pure or mixed, the measure of nonclassicality cannot be increased.

Operational Resource Theory (ORT)

ORT differs from RT in a way that in addition to the conditions met by resource measures, it captures the nonclassicality in operational terms i.e., it quantifies as to how much a useful quantum task can be performed by a state with no classical analogue.

Operational Resource Measure (ORM)

Wenchao et al., [23] have presented an ORM that not only satisfies the minimum conditions for RT; but also quantifies the ability of a pure state towards displacement sensing and provides a tight upper bound over the metrological power i.e. $N(\hat{\rho}) \geq W$. The ORM is defined as,

$$N(\hat{\rho}) := \min_{\{p_j, |\psi_j\rangle\}} \left[\max_{\mu} \left\{ \sum p_j \langle \psi_j | (\Delta \hat{X}_\mu)^2 | \psi_j \rangle \right\} \right] - \frac{1}{2},$$

where, $\hat{X}_\mu = \frac{i}{\sqrt{2}}(e^{-i\mu}\hat{a}^\dagger - e^{i\mu}\hat{a})$,

$$= \min_{\{p_j, |\psi_j\rangle\}} \left[\max_\mu \left\{ \sum p_j \left(\langle\psi_j|\hat{X}_\mu^2|\psi_j\rangle - \langle\psi_j|\hat{X}_\mu|\psi_j\rangle^2 \right) \right\} \right] - \frac{1}{2},$$

$$= \min_{\{p_j, |\psi_j\rangle\}} \left[\max_\mu \left\{ -\frac{1}{2} \sum p_j \left(\langle\psi_j|(e^{-2i\mu}\hat{a}^{\dagger 2} + e^{2i\mu}\hat{a}^2 - 2\hat{a}^\dagger\hat{a} - 1)|\psi_j\rangle \right. \right. \right.$$
$$\left. \left. \left. - \langle\psi_j|(e^{-i\mu}\hat{a}^\dagger - e^{i\mu}\hat{a})|\psi_j\rangle^2 \right) \right\} \right] - \frac{1}{2},$$

defining $\bar{n}_j = \langle\psi_j|\hat{a}^\dagger\hat{a}|\psi_j\rangle$, $\bar{\zeta}_j = \langle\psi_j|\hat{a}^2|\psi_j\rangle$, and $\bar{\alpha}_j = \langle\psi_j|\hat{a}|\psi_j\rangle$,

$$= \min_{\{p_j, |\psi_j\rangle\}} \left[\max_\mu \left\{ -\frac{1}{2} \sum p_j \left(e^{-2i\mu}(\bar{\zeta}_j^* - \bar{\alpha}_j^{*2}) + e^{2i\mu}(\bar{\zeta}_j - \bar{\alpha}_j^2) - 2\bar{n}_j - 1 \right. \right. \right.$$
$$\left. \left. \left. + 2|\bar{\alpha}_j|^2 \right) \right\} \right] - \frac{1}{2}.$$

Maximizing $N(\hat{\rho})$ with respect to μ leads to $\mu = 0, \pi/2$ and $\bar{\zeta}_j^* = \bar{\zeta}_j$, $\bar{\alpha}_j^{*2} = \bar{\alpha}_j^2$.

For $\mu = 0$,

$$N(\hat{\rho}) = \min_{\{p_j, |\psi_j\rangle\}} \left\{ -\sum p_j(\bar{\zeta}_j - \bar{\alpha}_j^2) + \sum p_j(\bar{n}_j - |\bar{\alpha}_j|^2) \right\}. \tag{4.2.6}$$

For $\mu = \pi/2$,

$$N(\hat{\rho}) = \min_{\{p_j, |\psi_j\rangle\}} \left\{ \sum p_j(\bar{\zeta}_j - \bar{\alpha}_j^2) + \sum p_j(\bar{n}_j - |\bar{\alpha}_j|^2) \right\}, \tag{4.2.7}$$

which for maximization to occur yield,

$$N(\hat{\rho}) = \min_{\{p_j, |\psi_j\rangle\}} \left\{ \left| \sum p_j(\bar{\zeta}_j - \bar{\alpha}_j^2) \right| + \sum p_j(\bar{n}_j - |\bar{\alpha}_j|^2) \right\}. \tag{4.2.8}$$

$N(\hat{\rho})$ can be written in a compact form using an extended state $\hat{\rho}_E = \sum_j p_j |\psi_j\rangle\langle\psi_j| \otimes |j\rangle_E\langle j|$ generated while using orthogonal vectors $|j\rangle_E$,

$$N(\hat{\rho}) = \min_{\{p_j, |\psi_j\rangle\}} \max_\mu F_{\hat{X}_\mu \otimes \hat{I}_E}(\hat{\rho}_E) - 1/2, \tag{4.2.9}$$

which follows from property of QFI, that, if second system of a bipartite $\hat{\rho}$ is traced out, then QFI of the resulting system cannot increase [48], i.e.,

$$F_{\hat{X}_\mu \otimes \hat{I}_E}(\hat{\rho}_E) \geq F_{\hat{X}_\mu}(Tr_E \hat{\rho}_E) = F_{\hat{X}_\mu}(\hat{\rho}), \tag{4.2.10}$$

$$\Rightarrow \min_{\{p_j, |\psi_j\rangle\}} \max_\mu F_{\hat{X}_\mu \otimes \hat{I}_E}(\hat{\rho}_E) = F_{\hat{X}_\mu}(\hat{\rho}).$$

For pure states ORM becomes,

$$N(\hat{\rho}) = \left| \bar{\zeta} - \bar{\alpha}^2 \right| + \bar{n} - |\bar{\alpha}|^2, \tag{4.2.11}$$

Conditions for Operationality of the Measure

Non-negativity, $N(\hat{\rho}) \geq 0$

- **For Classical States** For arbitrary classical state, i.e., a mixture of coherent states $\hat{\rho} = \sum p_j |\alpha_j\rangle\langle\alpha_j|$. Eq(4.2.8) yields,

$$N(\hat{\rho}) = \min_{\{p_j, |\psi_j\rangle\}} \left\{ \left| \sum p_j(\alpha_j^2 - \alpha_j^2) \right| + \sum p_j(|\alpha_j|^2 - |\alpha_j|^2) \right\},$$
$$= 0. \tag{4.2.12}$$

- **For Nonclassical States** From the decomposition of $\hat{\rho}$, at the minimum one of the state must be a nonclassical, i.e., $|\psi_j\rangle = |\psi_{NC}\rangle$, then using Cauchy-Schwarz inequality,

$$|\langle v|w\rangle| \leq \sqrt{\langle v|v\rangle\langle v|w\rangle}, \tag{4.2.13}$$

let $|w\rangle = \hat{a}|\psi_{NC}\rangle$ and $|v\rangle = |\psi_{NC}\rangle$,

$$|\langle\psi_{NC}|\hat{a}|\psi_{NC}\rangle| \leq \sqrt{\langle\psi_{NC}|\psi_{NC}\rangle\langle\psi_{NC}|\hat{a}^\dagger\hat{a}|\psi_{NC}\rangle},$$
$$|\bar{\alpha}_{NC}|^2 \leq \bar{n}_{NC} . \tag{4.2.14}$$

The equality sign will hold provided $|\psi_{NC}\rangle$ is an eigenstate of $\hat{a}$, which can only be true provided $|\psi_{NC}\rangle$ is a coherent state against the initial statement. Hence,

$$|\bar{\alpha}_{NC}|^2 < \bar{n}_{NC} \ . \tag{4.2.15}$$

Thus, from eq(4.2.8), for a nonclassical state,

$$N(\hat{\rho}) > 0. \tag{4.2.16}$$

Weak Monotonicity, $N(\wedge[\hat{\rho}]) \leq N(\hat{\rho})$

A linear optical operation/ map is defined as [49],

$$\wedge(\hat{\rho}) := Tr_A(U_L \hat{\rho} \otimes \hat{\rho}_A U_L^{\dagger}) = \sum_j q_j \sigma_j, \tag{4.2.17}$$

where, U_L is a unitary operator implemented through passive linear optical elements e.g. phase shifter, beam splitter and displacement operations with single mode, $\hat{\rho}_A$ is an ancilla classical state that is being traced out, $q_j = Tr(\Pi_j \hat{\rho}) = Tr(K_j \hat{\rho} K_j^{\dagger})$ is the probability of finding the system in mixed state σ_j, $\sigma_j = K_j \hat{\rho} K_j^{\dagger}/q_j = \sum_i p_i |\phi_{ij}\rangle\langle\phi_{ij}|$ are the post-measurement mixed states, K_j are Kraus/ detection operators and $\Pi_j = K_j^{\dagger} K_j$ are POVM elements already described. Eq(4.2.17) becomes,

$$\begin{aligned}
\wedge(\hat{\rho}) &= \sum_j q_j \left(K_j \hat{\rho} K_j^{\dagger}/q_j \right), \\
&= \sum_j K_j \hat{\rho} K_j^{\dagger}, \\
&= \sum_j K_j \left(\sum_i p_i |\psi_i\rangle\langle\psi_i| \right) K_j^{\dagger}, \\
&= \sum_{i,j} q_j p_i \left(\frac{K_j |\psi_i\rangle}{\sqrt{q_j}} \right) \left(\frac{\langle\psi_i| K_j^{\dagger}}{\sqrt{q_j}} \right), \\
&= \sum_{i,j} q_j p_i |\phi_{ij}\rangle\langle\phi_{ij}|. \tag{4.2.18}
\end{aligned}$$

Checking for weak monotonicity of $N(\hat{\rho})$,

$$N(\wedge(\hat{\rho})) = N\left(\sum_{i,j} q_j p_i |\phi_{ij}\rangle\langle\phi_{ij}| \right), \tag{4.2.19}$$

using eq(4.2.10),

$$\leq \max_{\mu} F_{\hat{X}_\mu \otimes \hat{I}_E \otimes \hat{I}_{A'}} \left(\sum_{i,j} q_j p_i |\phi_{ij}\rangle\langle\phi_{ij}| \otimes |i\rangle_E\langle i| \otimes |j\rangle_{A'}\langle j| \right) - \frac{1}{2},$$

where, $|j\rangle_{A'}$ is a classical ancilla state with mode A' and forms a set of orthogonal vectors $\{|j\rangle_{A'}\}$. Once again, linear optical mapping dictates that there exist a linear unitary and a classical ancilla state $\hat{\rho}_{AA'}$ such that, $Tr_A\left[U\hat{\rho}_E \otimes \hat{\rho}_{AA'} U^\dagger\right] = \sum_{i,j} q_j p_i |\phi_{ij}\rangle\langle\phi_{ij}| \otimes |i\rangle_E\langle i| \otimes |j\rangle_{A'}\langle j|$,

$$= \max_{\mu} F_{\hat{X}_\mu \otimes \hat{I}_E \otimes \hat{I}_{A'}} \left(Tr_A\left[U\hat{\rho}_E \otimes \hat{\rho}_{AA'} U^\dagger\right] \right) - \frac{1}{2},$$

$$\leq \max_{\mu} F_{\hat{X}_\mu \otimes \hat{I}_E \otimes \hat{I}_{AA'}} \left(U\hat{\rho}_E \otimes \hat{\rho}_{AA'} U^\dagger \right) - \frac{1}{2},$$

where, $\hat{\rho}_{AA'} = \sum_k r_k |\alpha_k\rangle\langle\alpha_k|$ is a coherent state in modes AA' with $\sum_k r_k = 1$,

$$= \max_{\mu} F_{\hat{X}_\mu \otimes \hat{I}_E \otimes \hat{I}_{AA'}} \left(U\hat{\rho}_E \otimes \sum_k r_k |\alpha_k\rangle\langle\alpha_k| U^\dagger \right) - \frac{1}{2},$$

using convexity of QFI i.e., $F_{\hat{X}_\mu}(\sum p_j |\psi_j\rangle\langle\psi_j|) \leq \sum p_j F_{\hat{X}_\mu}(|\psi_j\rangle\langle\psi_j|)$,

$$\leq \max_{\mu} \sum_k r_k F_{\hat{X}_\mu \otimes \hat{I}_E \otimes \hat{I}_{AA'}} \left(U\hat{\rho}_E \otimes |\alpha_k\rangle\langle\alpha_k| U^\dagger \right) - \frac{1}{2}.$$

Switching from Schrödinger to Heisenberg picture in quantum mechanics,

$$= \max_{\mu} \sum_k r_k F_{U^\dagger \hat{X}_\mu \otimes \hat{I}_E \otimes \hat{I}_{AA'} U} \left(\hat{\rho}_E \otimes |\alpha_k\rangle\langle\alpha_k| \right) - \frac{1}{2},$$

$$= \max_{\mu} \sum_k r_k F_{\hat{X}_\mu^U + \hat{X}_{AA'}^U} \left(\hat{\rho}_E \otimes |\alpha_k\rangle\langle\alpha_k| \right) - \frac{1}{2},$$

as QFI is additive under tensoring,

$$= \max_{\mu} \sum_k r_k \left\{ F_{\hat{X}_\mu^U}(\hat{\rho}_E) + F_{\hat{X}_{AA'}^U}(|\alpha_k\rangle\langle\alpha_k|) \right\} - \frac{1}{2},$$

$$= \max_{\mu} \left\{ F_{\hat{X}_\mu^U}(\hat{\rho}_E) + \sum_k r_k F_{\hat{X}_{AA'}^U}(|\alpha_k\rangle\langle\alpha_k|) \right\} - \frac{1}{2},$$

$$\leq \max_{\mu} F_{\hat{X}_\mu \otimes \hat{I}_E}(\hat{\rho}_E) - \frac{1}{2} = N(\hat{\rho}).$$

Hence,

$$N\big(\wedge(\hat{\rho})\big) \leq N(\hat{\rho}). \tag{4.2.20}$$

Convexity, i.e. $\sum_j p_j N(\hat{\rho}_j) \geq N(\sum_j p_j \hat{\rho}_j)$

We know that,

$$\sum_j p_j N(\hat{\rho}_j) = \sum_j p_j \left(\min_{\{p_j, |\psi_j\rangle\}} \max_{\mu} F_{\hat{X}_\mu \otimes \hat{I}_E}(\hat{\rho}_j \otimes |i\rangle_E\langle i|) - 1/2 \right),$$

$$= \min_{\{p_j, |\psi_j\rangle\}} \max_{\mu} \sum_j p_j F_{\hat{X}_\mu \otimes \hat{I}_E}(\hat{\rho}_j \otimes |i\rangle_E\langle i|) - 1/2,$$

using convexity of QFI,

$$\geq \min_{\{p_j, |\psi_j\rangle\}} \max_{\mu} F_{\hat{X}_\mu \otimes \hat{I}_E}(\sum_j p_j \hat{\rho}_j \otimes |i\rangle_E\langle i|) - 1/2,$$

as $\hat{\rho}_E = \sum_j p_j \hat{\rho}_j \otimes |i\rangle_E\langle i|$,

$$= \min_{\{p_j, |\psi_j\rangle\}} \max_{\mu} F_{\hat{X}_\mu \otimes \hat{I}_E}(\hat{\rho}_E) - 1/2,$$

$$= N(\sum_j p_j \hat{\rho}_j), \tag{4.2.21}$$

$$\Rightarrow \sum_j p_j N(\hat{\rho}_j) \geq N(\hat{\rho}). \tag{4.2.22}$$

$$N(\hat{\rho}) = \min_{\{p_j, |\psi_j\rangle\}} \max_\mu F_{\hat{X}_\mu \otimes \hat{I}_E}(\hat{\rho}_E) - 1/2,$$

$$\geq \min_{\{p_j, |\psi_j\rangle\}} \max_\mu F_{\hat{X}_\mu} \{Tr_E(\hat{\rho}_E)\} - 1/2,$$

$$= \max_\mu F_{\hat{X}_\mu}(\hat{\rho}) - 1/2,$$

$$= W(\hat{\rho}),$$

$$\Rightarrow N(\hat{\rho}) \geq W(\hat{\rho}), \tag{4.2.23}$$

where, equality holds for pure state. Thus, for a pure state, metrological power for displacement measurement can be found using Eq. (4.2.11), i.e.,

$$N(\hat{\rho}) = W_{\hat{X}}(\hat{\rho}) = \bar{n} - |\bar{\alpha}|^2 + \left|\bar{\zeta} - \bar{\alpha}^2\right|. \tag{4.2.24}$$

where, $\bar{\alpha} = \langle\psi|\hat{a}|\psi\rangle$, and $\bar{\zeta} = \langle\psi|\hat{a}^2|\psi\rangle = \alpha^2$.

4.3 Metrological Power of Cats

In this section, we have analytically worked out the metrological power of cats for quadrature and phase sensing.

4.3.1 Quadrature Sensing

For quadrature sensing, we have evaluated the expectation values of different operators involved in eq. (4.2.24) for our probe states and worked out their metrological power.

2H Cats

Metrological power for even cats $W_{\hat{X}}^e$ becomes,

$$W_{\hat{X}}^e = \frac{2|\alpha|^2}{1 + e^{-2|\alpha|^2}}, \tag{4.3.1}$$

and for odd cats,

$$W_{\hat{X}}^o = \frac{2|\alpha|^2}{1 - e^{-2|\alpha|^2}}, \tag{4.3.2}$$

55

where, $\bar{\alpha} = 0$ and $\bar{\zeta} = \alpha^2$ for even and odd cats both. For YS cats, the metrological power is given as,

$$W_{\hat{X}}^{ys} = |\alpha|^2 - |\alpha|^2 e^{-4|\alpha|^2} + |\alpha^2 + \alpha^2 e^{-4|\alpha|^2}|,$$

which for real α reduces to,

$$= 2\alpha^2, \tag{4.3.3}$$

with $\bar{\alpha} = -i\alpha e^{-2|\alpha|^2}$ and $\bar{\zeta} = \alpha^2$.

3H Cats

The metrological power for 3H cats is,

$$W_{\hat{X}}^{3h} = \frac{N_{3h}^2 |\alpha|^2}{N_o^2} + \alpha^2 N_{3h}^2 [1/N_e^2 + 2e^{-|\alpha|^2/2}],$$
$$= 2|\alpha|^2 N_{3h}^2 [2 + e^{-|\alpha|^2/2}], \tag{4.3.4}$$

which is obtained via following averages, with use of identities $\langle 1|\alpha\rangle = \alpha e^{-|\alpha|^2/2}$ and $\langle 2|\alpha\rangle = \frac{\alpha^2}{\sqrt{2}} e^{-|\alpha|^2/2}$,

$$\bar{\alpha} = 0. \tag{4.3.5}$$
$$\bar{\zeta} = \alpha^2 N_{3h}^2 [1/N_e^2 + 2e^{-|\alpha|^2/2}]. \tag{4.3.6}$$

4H Cats Evaluating various averages involved in $W_{\hat{X}}$ for 4H cats,

$$\bar{\alpha} = -i\alpha e^{-|\alpha|^2} (\cos|\alpha|^2 - \sin|\alpha|^2). \tag{4.3.7}$$
$$\bar{\zeta} = \alpha^2 e^{-2|\alpha|^2}. \tag{4.3.8}$$

Metrological power becomes,

$$W_{\hat{X}}^{4h} = |\alpha|^2 + |\alpha|^2 e^{-2|\alpha|^2} \left[1 - (\cos|\alpha|^2 - \sin|\alpha|^2)^2 + e^{-2|\alpha|^2} (\cos|\alpha|^2 - \sin|\alpha|^2)^2\right]. \tag{4.3.9}$$

Excited 2H Cat

For excited even cats, metrological power becomes,

$$W_{\hat{X}}^{eec} = N_{eec}^2\big[1 + 4N_e^2|\alpha|^2(|\alpha|^2 + 3)\big], \tag{4.3.10}$$

with $\bar{\alpha} = 0$ and $\bar{\zeta} = N_{eec}^2\alpha^2(3 + |\alpha|^2\frac{N_e^2}{N_o^2})$ Whereas for excited odd cats, $W_{\hat{X}}$ is given by,

$$W_{\hat{X}}^{eoc} = N_{eoc}^2\big[1 + 4N_o^2|\alpha|^2(|\alpha|^2 + 3)\big], \tag{4.3.11}$$

with corresponding averages $\bar{\alpha} = 0$ and $\bar{\zeta} = N_{eoc}^2\alpha^2(3 + |\alpha|^2\frac{N_o^2}{N_e^2})$. Metrological power for YS states simplifies to,

$$W_{\hat{X}}^{eys} = N_{eys}^4\big(1 + 7|\alpha|^2 + 8|\alpha|^4 + 2|\alpha|^6\big), \tag{4.3.12}$$

with none of the averages vanishing, i.e.,

$$\bar{\alpha} = iN_{eys}^2\alpha(-2 + |\alpha|^2). \tag{4.3.13}$$

$$\bar{\zeta} = N_{eys}^2\big(3\alpha^2 + \alpha^2|\alpha|^2\big). \tag{4.3.14}$$

Excited 3H Cats

For 3H cats,

$$W_{\hat{X}}^{e3h} = N_{e3h}^2\big[1 + 2N_{3h}^2|\alpha|^2(6 + 2|\alpha|^2 + 3e^{-|\alpha|^2/2})\big], \tag{4.3.15}$$

with $\bar{\alpha} = 0$ and $\bar{\zeta} = N_{e3h}^2N_{3h}^2\alpha^2\big[\frac{3}{N_e^2} + 6e^{-|\alpha|^2/2} + 2|\alpha|^2(1 - e^{-2|\alpha|^2})\big]$.

Excited 4H Cats

Evaluating various averages involved in W_X,

$$\bar{\alpha} = iN_{e4h}^2\alpha e^{-|\alpha|^2}\big[|\alpha|^2(\cos|\alpha|^2 + \sin|\alpha|^2) - 2(\cos|\alpha|^2 - \sin|\alpha|^2)\big]. \tag{4.3.16}$$

$$\bar{\zeta} = N_{e4h}^2\alpha^2 e^{-2|\alpha|^2}(3 - |\alpha|^2). \tag{4.3.17}$$

Metrological power becomes,

$$W_{\hat{X}}^{e4h} = N_{e4h}^4 \left[1 + 4|\alpha|^2 + 4|\alpha|^4 + |\alpha|^6 - |\alpha|^2 e^{-2|\alpha|^2} (|\alpha|^4 - 2|\alpha|^2 - 3) \right]. \qquad (4.3.18)$$

4.3.2 Phase Sensing

Recalling Eq. (4.2.5), for metrological power of states for phase sensing and simplifying it further,

$$\begin{aligned} W_{\hat{n}} &= F_n(|\psi\rangle) - |\alpha|^2 \\ &= \langle\psi|(\Delta\hat{n})^2|\psi\rangle - |\alpha|^2, \\ &= \langle\hat{a}^\dagger\hat{a}\rangle + \langle\hat{a}^{\dagger 2}\hat{a}^2\rangle - \langle\hat{a}^\dagger\hat{a}\rangle^2 - |\alpha|^2. \end{aligned} \qquad (4.3.19)$$

All the averages involved in the above equation have already been worked out. Foregoing in view, the metrological power for cats in estimating phase are given as under:

Even Cats

$$\begin{aligned} W_{\hat{n}}^e &= |\alpha|^2 N_e^2/N_o^2 + |\alpha|^4 - |\alpha|^4 N_e^4/N_o^4 - |\alpha|^2, \\ &= 4|\alpha|^2 N_e^2 e^{-2|\alpha|^2} (4|\alpha|^2 N_e^2 - 1). \end{aligned}$$

Odd Cat

$$\begin{aligned} W_{\hat{n}}^o &= |\alpha|^2 N_o^2/N_e^2 + |\alpha|^4 - |\alpha|^4 N_o^4/N_e^4 - |\alpha|^2, \\ &= 4|\alpha|^2 N_o^2 e^{-2|\alpha|^2} (1 - 4|\alpha|^2 N_o^2). \end{aligned}$$

YS States

$$\begin{aligned} W_{\hat{n}}^{ys} &= |\alpha|^2 + |\alpha|^4 - |\alpha|^4 - |\alpha|^2, \\ &= 0. \end{aligned}$$

3H Cats

$$W_{\hat{n}}^{3h} = \frac{N_{3h}^2 |\alpha|^2}{N_o^2} + \frac{N_{3h}^2 |\alpha|^4}{N_e^2} - \frac{N_{3h}^4 |\alpha|^4}{N_o^4} - |\alpha|^2,$$

$$= N_{3h}^2 |\alpha|^2 \left[\frac{1}{N_o^2} + \frac{|\alpha|^2}{N_e^2} - \frac{N_{3h}^2 |\alpha|^2}{N_o^4} \right] - |\alpha|^2.$$

4H Cats

$$W_{\hat{n}}^{4h} = |\alpha|^2 + |\alpha|^4 - |\alpha|^4 - |\alpha|^2,$$

$$= 0.$$

YS and 4H state hold no metrological power in phase sensing; whereas, the rest of cats do.

For excited cats, the expressions for the quantifier are relatively complex, with none showing lack of ability of enhancing metrology.

Excited Even Cat

$$W_{\hat{n}}^{eec} = N_{eec}^2 \left(1 + 3|\alpha|^2 \frac{N_e^2}{N_o^2} + |\alpha|^4 \right) + N_{eec}^2 \left[4|\alpha|^2 \frac{N_e^2}{N_o^2} + 5|\alpha|^4 + |\alpha|^6 \frac{N_e^2}{N_o^2} \right]$$

$$- N_{eec}^4 \left(1 + 3|\alpha|^2 \frac{N_e^2}{N_o^2} + |\alpha|^4 \right)^2 - |\alpha|^2,$$

$$= N_{eec}^4 |\alpha|^2 \left[-16 N_e^4 |\alpha|^6 e^{-2|\alpha|^2} + \frac{N_e^2}{N_o^2} \left(|\alpha|^4 - 2|\alpha|^2 \frac{N_e^2}{N_o^2} + 2 \right) + 4|\alpha|^2 \right] - |\alpha|^2.$$

Excited Odd Cats

$$W_{\hat{n}}^{eoc} = N_{eoc}^2 \left(1 + 3|\alpha|^2 \frac{N_o^2}{N_e^2} + |\alpha|^4 \right) + N_{eoc}^2 \left[4|\alpha|^2 \frac{N_o^2}{N_e^2} + 5|\alpha|^4 + |\alpha|^6 \frac{N_o^2}{N_e^2} \right]$$

$$- N_{eoc}^4 \left(1 + 3|\alpha|^2 \frac{N_o^2}{N_e^2} + |\alpha|^4 \right)^2 - |\alpha|^2,$$

$$= N_{eoc}^4 |\alpha|^2 \left[16 N_o^4 |\alpha|^6 e^{-2|\alpha|^2} + \frac{N_o^2}{N_e^2} \left(|\alpha|^4 - 2|\alpha|^2 \frac{N_o^2}{N_e^2} + 2 \right) + 4|\alpha|^2 \right] - |\alpha|^2.$$

Excited YS States

$$W_{\hat{n}}^{eys} = N_{eys}^4 |\alpha|^2 (2 + 2|\alpha|^2 + |\alpha|^4) - |\alpha|^2.$$

Excited 3H Cats

$$W_{\hat{n}}^{e3h} = N_{e3h}^4 N_{3h}^4 |\alpha|^2 \big[44 + 16|\alpha|^2 + 6|\alpha|^4 + e^{-|\alpha|^2/2}(32|\alpha|^2 - 16 + 8|\alpha|^4)$$
$$+ e^{-2|\alpha|^2}(-4 + 56|\alpha|^2 - 2|\alpha|^4 - 16|\alpha|^6) + e^{-5|\alpha|^2/2}(-16 + 32|\alpha|^2 - 8|\alpha|^4)$$
$$+ e^{-4|\alpha|^2}(-8 + 8|\alpha|^2 - 4|\alpha|^4) \big] - |\alpha|^2.$$

Excited 4H Cats

$$W_{\hat{n}}^{e4h} = N_{e4h}^4 |\alpha|^2.$$

Chapter 5

Results and Discussion

Mandel Q parameter, that reflects the photon statistics of a state, helps in quantifying the nonclassicality of states; while, the metrological power seeks to quantify it operationally, i.e., how much of a quantum task can be performed by a state. A possibility exist where Q parameter could identify the states which are metrologically strong. Furthermore, in chapter 4 it was seen that free operations do not enhance metrology of a state. In contrast, addition of a photon to a state generates entanglement of signal and idler mode of a state through spontaneous parametric down conversion and is therefore not considered as a free operation. Thus, it will lead to enhancing metrology. However, it remains to be seen that how much it could increase the metrological power of cats.

In this chapter, we will carry out an analysis of the results through comparison via graphs focusing on following two aspects, (within the purview of cats):

- whether Mandel Q parameter serves as an indicator of enhanced metrology of states irrespective of the generator or otherwise,

- impact of addition of photon on the Q parameter and metrological power of states.

5.1   Mandel Q-parameter Vs Metrology

In this sub-section, comparison of Q parameter of states vis-à-vis their metrological power (quadrature and phase sensing) has been drawn.

Schödinger Cats and YS State

From Wigner functions of all the cats worked out in chapter 3, we know that these states are nonclassical; however, Q parameter as evident from fig.5.1.1 reveals different picture. Fig.5.1.1 (a) indicates that only odd states show nonclassical behaviour without ambiguity. Q parameter for YS identifies it as classical states; whereas for even state it is ambiguous as to whether they are classical or nonclassical. Fig.5.1.1(b) indicate that odd state enjoys enhanced metrology for displacement sensing, which is so far in consonance with Q parameter. For YS state, despite that Q parameter identified it as classical, it shows non-zero metrological power and even state which could not be classified as classical or nonclassical has the least metrological power among all three states. The same figure's third plot (c) that shows the trend of metrological power of the subject cats for phase sensing indicate that only even cat possess some metrological power; whereas odd cat and YS state have none. Thus, Q is neither capturing the full extent of nonclassicality of these states nor their ability in enhancing metrology.
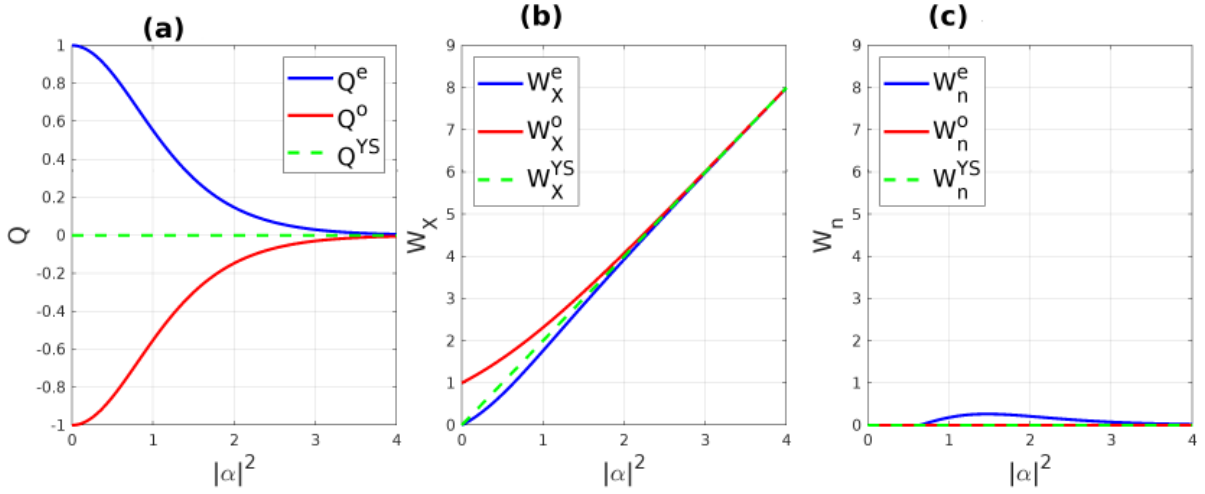
Figure 5.1.1: Comparison of photon statistics and metrological power of even, odd and YS cat states for real α. (a) Plot of Q Vs $|\alpha|^2$. Among all three states, Q only identifies odd cat as nonclassical. (b) Plot of W_X Vs $|\alpha|^2$ and (c) W_n Vs $|\alpha|^2$. The last two graphs reflect that odd cat has enhanced metrology for displacement sensing and even cat for phase.

3H and 4H Cats

3H and 4H cat states, both, are non-classical which gets evident from their Wigner functions whereas Q parameter (Fig.5.1.2(a)) does not clearly reflect nonclassicality of the two states. 4H cat state is tagged as classical; whereas Q fails to clearly identify 3H cat as

nonclassical, for these states exhibit super-Poissonian photon statistics. Fig.5.1.2(b) and (c) dictate that 4H cat is relatively strong from metrological point of view for displacement sensing than 3H up to certain value of $|\alpha|^2$ after which 3H is stronger, and for phase sensing 4H offers no metrological advantage.
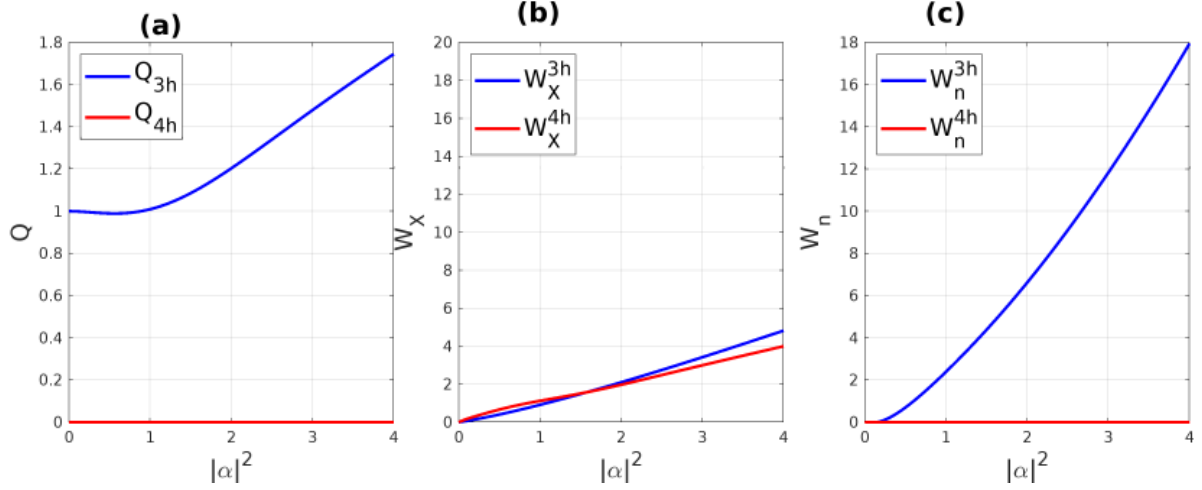
Figure 5.1.2: Comparison of Q and metrological power for displacement and phase sensing of 3H and 4H cats for real α. (a), (b) and (c) are plots of Q, W_X and W_n Vs $|\alpha|^2$ respectively. (a) reflect that only $Q_{3h} > 0$ with super-Poissonian statistics for 3H state, and Poissonian for 4H cat state. (b) and (c) show the relative metrological strength 3H state enjoys for phase over 4H cat, with reversed strength up to a point for displacement sensing.

Above analysis of various plots of Q-parameter and metrological powers of states clearly reflect that Q-parameter cannot be identified as an indicator for metrological strength of a state.

5.2 Impact of Photon Addition

In this subsection, the impact of photon addition has been explored on nonclassicality of various cat states, both in terms of overall nonclassicality and useful nonclassicality through their metrological power.

Consider the following comparison of Q, W_X and W_n for various cat states before and after photon addition, for real α.

Even Cat

Figure 5.2.1: Comparing Q (a), metrological power for displacement W_X (b) and phase sensing W_n (c) of even and excited even state for real α. (a) The super-Poissonian character of even cat switches to sub-Poissonian for its excited form reflecting increase in nonclassicality. (b) and (c) reveals increased metrology of excited even cat in displacement and phase sensing.

Fig. 5.2.1 (a) reflect that even though Q parameter was ambiguous about nonclassicality of even cat, due to positive values of Q indicating super-Poissonian photon statistics; the excited even is clearly nonclassical. Thus, addition of a photon to even cat has transformed the state into a state that now shows sub-Poissonian statistics. Fig. 5.2.1 (b) and (c) shows the resulting state has enhanced metrology in displacement as well as phase sensing.
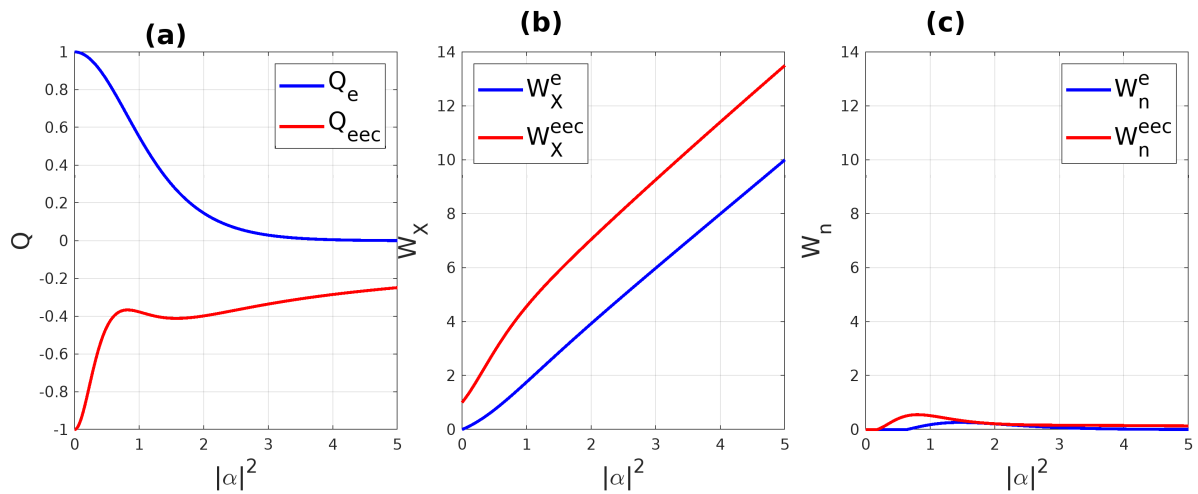
Odd Cat

Figure 5.2.2: Comparing Q (a), metrological power for displacement W_X (b) and phase sensing W_n (c) of odd and excited odd state for real α. (a) The sub-Poissonian character of excited odd cat is more stronger than odd cat showing reflecting increase in nonclassicality. (b) and (c) reveals increased metrology of excited odd cat in displacement and phase sensing.

Fig 5.2.2 (a) reveals increased nonclassicality of excited odd cat as the curve representing Q values has shifted further below towards more negative values of Q. This shows that excited odd cats have smaller variance in photon number in comparison to mean than for its non-excited counterpart. Fig 5.2.2 (b) and (c) shows enhanced metrology of excited odd cat in displacement and phase sensing respectively.

YS State

Fig 5.2.3 (a) shows that unlike YS state, Q parameter identifies excited YS state as nonclassical as $Q_{eys} < 0$ revealing the underlying sub-Poissonian photon statistics of this state. Whereas, fig. 5.2.3 (b) and (c), as in previous two cases indicate enhanced metrology of the excited cat.

Figure 5.2.3: Comparing Q (a), metrological power for displacement W_X (b) and phase sensing W_n (c) of YS and excited YS state for real α. (a) The Poissonian character of YS state switches to sub-Poissonian for its excited form reflecting increase in nonclassicality. (b) and (c) reveals increased metrology of excited YS cat in displacement and phase sensing.
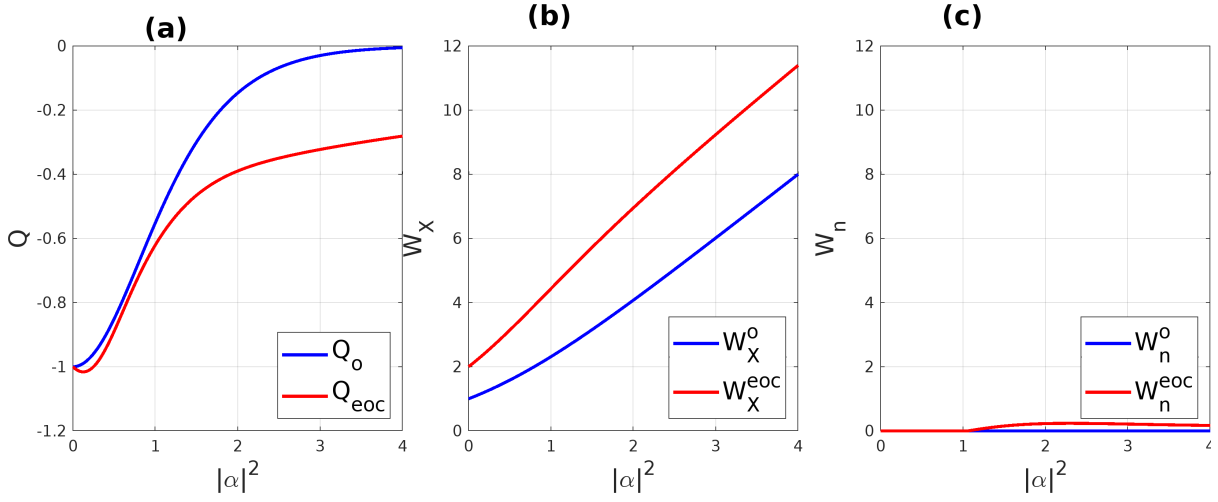
3H Cat

Figure 5.2.4: Comparing Q (a), metrological power for displacement W_X (b) and phase sensing W_n (c) of even and excited even state for real α. (a) The super-Poissonian character of 3H cat switches to sub-Poissonian for its excited form reflecting increase in nonclassicality. (b) and (c) reveals increased metrology of excited cat in displacement and phase sensing.

From fig 5.2.2 (a) it is evident that even though Q could not clearly identify 3H cat as nonclassical due to super-Poissonian nature of its photon statistics, the negative values of Q_{e3H} reflects underlying sub-Poissonian statistics and thus reveals that excited 3H cat is nonclassical. Fig 5.2.2 (b) and (c) shows enhanced metrology of excited odd cat in displacement and phase sensing respectively.
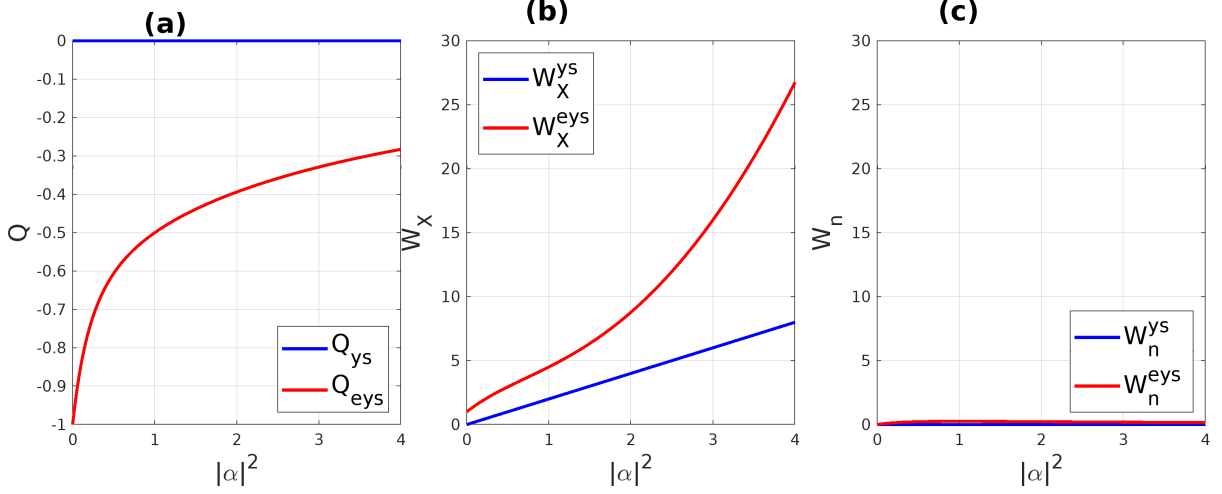
4H Cat

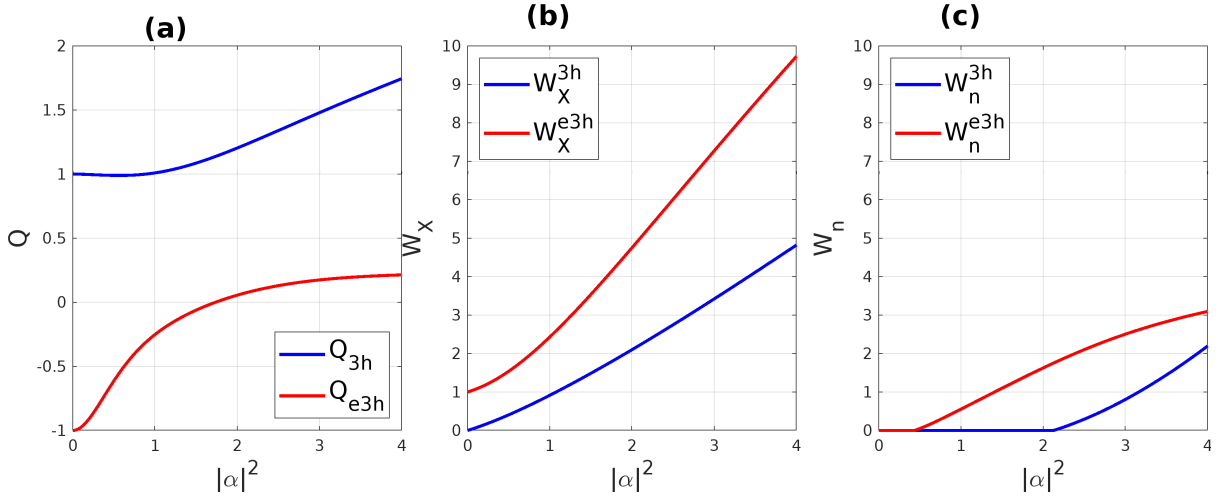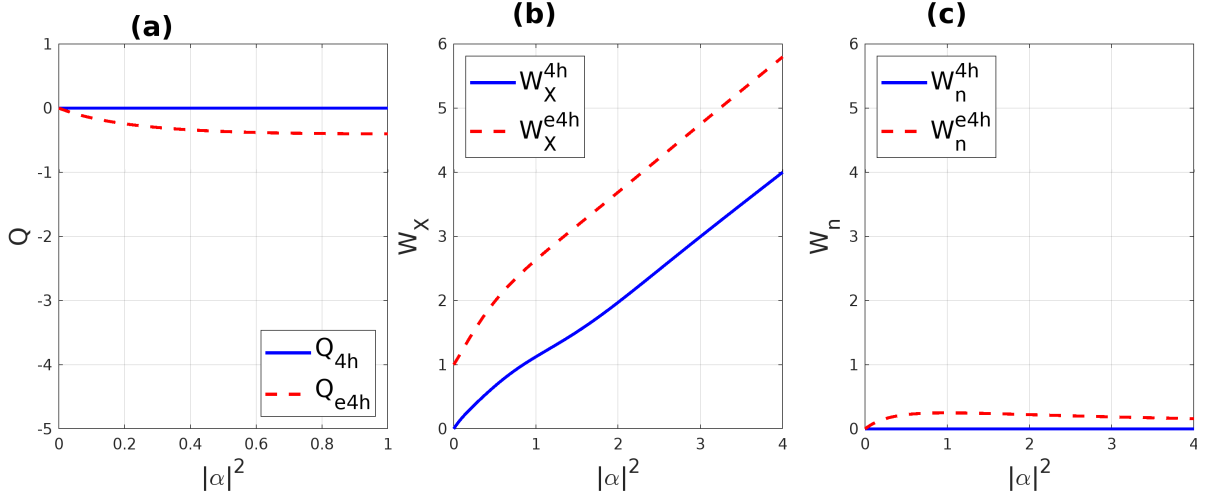**Figure 5.2.5:** Comparing Q (a), metrological power for displacement W_X (b) and phase sensing W_n (c) of 4H and excited 4H cat for real α. (a) The Poissonian character of 4H cat switches to sub-Poissonian for its excited form reflecting increase in nonclassicality. (b) and (c) reveals increased metrology of excited 4H cat.

Fig 5.2.5 depicts same phenomena as for YS state. Fig. (a) shows that even though 4H cat is dubbed as classical due to $Q_{ys} = 0$, after photon addition the resulting excited state has been identified as nonclassical as $Q_{eys} < 0$ revealing its sub-Poissonian photon statistics. Fig 5.2.5 (b) and (c) reflects enhanced metrology for excited 4H irrespective of the generator used.

For all the states, photon addition enhances the overall nonclassicality of states as well as enhance their metrological strength irrespective of the generator used. Hence, addition of photon adds to the nonclassicality of the states.

Chapter 6

Summary and Conclusion

Our work substantially explores the nonclassicality of a particular form of quantum states, through various quantifiers, with significance towards enhancing quantum metrology. The probe states considered for this study were mainly Schödinger cat states, which hold a unique place in quantum optics owing to their origin from Schödinger gedanken experiment in 1935, actually meant to critique probabilistic interpretation of wave function i.e., superposition of microscopic states. Appreciating the cats as superposition of distinct coherent states, the study was also extended to states with similar construction i.e., superposition of number of coherent states with distinct phases resulting in multi-headed cat states. The quantifiers used for detail examination of nonclassicality of the cat states, have been worked out analytically. These include Wigner function, Mandel Q parameter, metrological power and operational resource measure. All of these quantifiers capture various attributes of nonclassicality of the states, where the later two seek to capture the utility of nonclassical states as a resource in enhancing quantum tasks and can be considered as operational quantifiers of nonclassicality. Two research questions were posited during the course of this study, one out of which considered the significance of Q parameter as indicator of relative metrological power of states across estimation of different classical parameters. To answer this question, we graphically compared the results obtained for the Mandel Q parameter and metrological power in sensing phase and displacement in phase space, of our probe states . We observe that the Q parameter does not predict trends in metrology of phase and displacement.

Next, we have also explored as to whether quantum metrology of the Schödinger cats can be enhanced by forming excited cats, as the process that entails forming such cats

is known to add to the nonclassical characteristics of a state. To test the proposition, excited cats were realized by adding a single photon to the cats, which in lab translates to spontaneous down conversion of a single photon to an entangled pair, in signal and idler mode, and driving the cat state in signal mode through this converter. The detail schematics of the experimental setup was devised and presented in this study. The results thus obtained in seeking the impact of photon addition to the cats in enhancing metrology were promising as we observed increment in metrological power across all the cats and parameters with no exceptions.

An important question that can further this study, is consideration of metrological power of cats for double mode interferometry using Mach-Zehnder Interferometer. The reader, can also explore the metrology of cats by exploiting entanglement and multiple photon addition.

Appendix A

Appendix to Chapter 2

A.1 Non-orthogonality of Coherent States

$$\langle\lambda|\gamma\rangle = (e^{-|\lambda|^2/2}\sum_{m=0}^{\infty}\frac{\lambda^{*m}}{\sqrt{m!}}\langle m|)(e^{-|\gamma|^2/2}\sum_{n=0}^{\infty}\frac{\gamma^n}{\sqrt{n!}}|n\rangle)$$

$$= e^{-(|\lambda|^2+|\gamma|^2)/2}[\sum_{n=0}^{\infty}\frac{(\lambda^*\gamma)^n}{n!}]$$

$$= e^{-(|\lambda|^2+|\gamma|^2)/2}e^{\lambda^*\gamma} \qquad\qquad (A.1.1)$$

$$= e^{-(|\lambda|^2+|\gamma|^2-2\lambda^*\gamma+\lambda\gamma^*-\lambda\gamma^*)/2}$$

$$= e^{-(|\lambda-\gamma|^2-\lambda^*\gamma+\lambda\gamma^*)/2}$$

$$= e^{-(|\lambda-\gamma|)^2/2}e^{(\lambda^*\gamma-\lambda\gamma^*)/2}$$

A.2 Normalization of Coherent States

$$\int|\lambda\rangle\langle\lambda|d^2\lambda = \int e^{-|\lambda|^2}\sum_{m=0}^{\infty}\sum_{n=0}^{\infty}\frac{\lambda^n}{\sqrt{n!}}\frac{\lambda^{*m}}{\sqrt{m!}}|n\rangle\langle m|d^2\lambda$$

using polar form of λ, i.e., $\lambda = se^{i\theta}$, $d^2\lambda = sdsd\theta$ where $s \in [o,\infty]$ and $\theta \in [0,2\pi]$

$$= \sum_{m=0}^{\infty}\sum_{n=0}^{\infty}\int e^{-s^2}\frac{s^{n+m+1}}{\sqrt{n!m!}}e^{i(n-m)\theta}|n\rangle\langle m|dsd\theta$$

$$= \sum_{m=0}^{\infty}\sum_{n=0}^{\infty}\frac{|n\rangle\langle m|}{\sqrt{n!m!}}\int_0^{\infty}e^{-s^2}s^{n+m+1}ds\int_0^{2\pi}e^{i(n-m)\theta}d\theta$$

using the orthogonality condition for complex exponential function, $\int_0^{2\pi} e^{i(n-m)\theta} = 2\pi\delta_{nm}$, and eliminating index m through contraction due to Kronecker delta,

$$= \pi \sum_{n=0}^{\infty} \frac{|n\rangle\langle n|}{n!} \int_0^{\infty} e^{-s^2}(s^2)^n(2sds)$$

which by introducing variable change as $s^2 = t$ and $2sds = dt$, yields,

$$= \pi \sum_{n=0}^{\infty} \frac{|n\rangle\langle n|}{n!} \int_0^{\infty} e^{-t}t^n dt$$

the integral using definition of Gamma function equates to $n!$

$$= \pi \sum_{n=0}^{\infty} |n\rangle\langle n|$$

exploiting completeness of number states,

$$= \pi \tag{A.2.1}$$

A.3 Generating Coherent State through Displacement Operator

$$\hat{D}(\lambda)|0\rangle = e^{\lambda\hat{a}^\dagger - \lambda^*\hat{a}}|0\rangle$$

Using disentangling theorem, $e^{A+B} = e^A e^B e^{-[A,B]/2}$ with $A = \lambda\hat{a}^\dagger$ and $B = -\lambda^*\hat{a}$, above equation yields,

$$= e^{\lambda\hat{a}^\dagger} e^{-\lambda^*\hat{a}} e^{-|\lambda|^2/2}|0\rangle$$

using Taylor expansion for exponential functions,

$$= e^{-|\lambda|^2/2}(\sum_{n=0}^{\infty}\frac{(\lambda\hat{a}^\dagger)^n}{n!})(\sum_{m=0}^{\infty}\frac{(-\lambda^*\hat{a})^m}{m!})|0\rangle$$

$$= e^{-|\lambda|^2/2}(\sum_{n=0}^{\infty}\frac{(\lambda\hat{a}^\dagger)^n}{n!})(1+\sum_{m=1}^{\infty}\frac{(-\lambda^*\hat{a})^m}{m!})|0\rangle$$

As $\hat{a}|0\rangle = 0$,

$$= e^{-|\lambda|^2/2}\sum_{n=0}^{\infty}\frac{(\lambda\hat{a}^\dagger)^n}{n!}|0\rangle$$

$$= e^{-|\lambda|^2/2}\sum_{n=0}^{\infty}\frac{\lambda^n}{\sqrt{n!}}|n\rangle$$

$$= |\lambda\rangle \tag{A.3.1}$$

Appendix B

Appendix to Chapter 3

B.1 Wigner Function for Even Cat

$$W_e(\beta) = \frac{1}{\pi^2} \int d^2\lambda e^{\lambda^*\beta - \lambda\beta^*} |N_e|^2 [e^{\lambda\alpha^* - \lambda^*\alpha}$$

$$+ e^{-(\lambda\alpha^* - \lambda^*\alpha)} + e^{-2|\alpha|^2}(e^{\lambda\alpha^* + \lambda^*\alpha} + e^{-(\lambda\alpha^* + \lambda^*\alpha)})] e^{-|\lambda|^2/2}$$

Let's take $\alpha = \frac{\alpha_r + i\alpha_i}{\sqrt{2}}$, $\beta = \frac{\beta_r + i\beta_i}{\sqrt{2}}$ and $\lambda = \frac{\lambda_r + i\lambda_i}{\sqrt{2}}$ then $d^2\lambda = d\lambda_r d\lambda_i/2$,

$$= \frac{|N_e|^2}{2\pi^2} \int d\lambda_r d\lambda_i e^{i(\beta_i\lambda_r - \beta_r\lambda_i)} [e^{i(\alpha_r\lambda_i - \alpha_i\lambda_r)} + e^{-i(\alpha_r\lambda_i - \alpha_i\lambda_r)}$$

$$+ e^{-(\alpha_r^2 + \alpha_i^2)}(e^{\alpha_r\lambda_r + \alpha_i\lambda_i} + e^{(\alpha_r\lambda_r + \alpha_i\lambda_i)})] e^{\frac{-1}{4}(\lambda_r^2 + \lambda_i^2)}$$

$$= \frac{|N_e|^2}{2\pi^2} \left[\left(\int d\lambda_r e^{\frac{-\lambda_r^2}{4}} e^{i(\beta_i - \alpha_i)\lambda_r} \right) \left(\int d\lambda_i e^{\frac{-\lambda_i^2}{4}} e^{-i(\beta_r - \alpha_r)\lambda_i} \right) \right.$$

$$+ \left(\int d\lambda_r e^{\frac{-\lambda_r^2}{4}} e^{i(\beta_i + \alpha_i)\lambda_r} \right) \left(\int d\lambda_i e^{\frac{-\lambda_i^2}{4}} e^{-i(\beta_r + \alpha_r)\lambda_i} \right)$$

$$+ e^{-(\alpha_r^2 + \alpha_i^2)} \left(\int d\lambda_r e^{\frac{-\lambda_r^2}{4}} e^{(\alpha_r + i\beta_i)\lambda_r} \right) \left(\int d\lambda_i e^{\frac{-\lambda_i^2}{4}} e^{(\alpha_i - i\beta_r)\lambda_i} \right)$$

$$+ e^{-(\alpha_r^2 + \alpha_i^2)} \left. \left(\int d\lambda_r e^{\frac{-\lambda_r^2}{4}} e^{-(\alpha_r - i\beta_i)\lambda_r} \right) \left(\int d\lambda_i e^{\frac{-\lambda_i^2}{4}} e^{-(\alpha_i + i\beta_r)\lambda_i} \right) \right]$$

using standard gaussian integral,

$$
= \frac{4\pi|N_e|^2}{2\pi^2} \left[e^{-(\beta_i-\alpha_i)^2} e^{-(\beta_r-\alpha_r)^2} + e^{-(\beta_i+\alpha_i)^2} e^{-(\beta_r+\alpha_r)^2} \right.
$$
$$
\left. + e^{-(\alpha_r^2+\alpha_i^2)} \left(e^{(\alpha_r+i\beta_i)^2} e^{(\alpha_i-i\beta_r)^2} + e^{(\alpha_r-i\beta_i)^2} e^{(\alpha_i+i\beta_r)^2} \right) \right]
$$
$$
= \frac{2|N_e|^2}{\pi} \left[e^{-2(|\beta|^2+|\alpha|^2-\alpha\beta^*-\alpha^*\beta)} + e^{-2(|\beta|^2+|\alpha|^2+\alpha\beta^*+\alpha^*\beta)} \right.
$$
$$
\left. + e^{-2|\alpha|^2} \left(e^{2(|\alpha|^2-|\beta|^2-\alpha\beta^*+\alpha^*\beta)} + e^{2(|\alpha|^2-|\beta|^2+\alpha\beta^*-\alpha^*\beta)} \right) \right]
$$
$$
= \frac{2|N_e|^2}{\pi} \left[e^{-2|\beta-\alpha|^2} + e^{-2|\beta+\alpha|^2} + e^{-2|\beta|^2} \left(e^{-2(\alpha\beta^*-\alpha^*\beta)} + e^{2(\alpha\beta^*-\alpha^*\beta)} \right) \right]
$$
$$
W_e(\beta) = \frac{2|N_e|^2}{\pi} \left[e^{-2|\beta-\alpha|^2} + e^{-2|\beta+\alpha|^2} + 2e^{-2|\beta|^2} \cos 2i(\alpha\beta^* - \alpha^*\beta) \right] \qquad \text{(B.1.1)}
$$

Appendix C

Appendix to Chapter 4

C.1 Derivation of CRB

For $N = 1$, the CRB is given as,

$$\Delta^2 \Phi \geq \frac{1}{F(\phi)} \tag{C.1.1}$$

The derivation of CRB is a direct result of application of Cauchy-Schwarz Inequality. For a PDF $p(\mu|\phi)$ that gives the conditional probability of observing readout μ, for given value of ϕ, the average of an estimator $\Phi(\mu)$ is given as,

$$\langle \Phi(\mu) \rangle = \int p(\mu|\phi)\Phi(\mu)d\mu$$

and the inner product of $\Phi(\mu)$ with $\partial_\phi L(\mu|\phi)$ is defined as,

$$\langle \Phi(\mu)\partial_\phi L(\mu|\phi) \rangle = \int d\mu f(\mu)\Phi(\mu)\partial_\phi L(\mu|\phi)$$

The covariance between two functions $\Phi(\mu)$ and $\partial_\phi L(\mu|\phi)$ is defined as,

$$Cov[\phi, \partial_\phi L(\mu|\phi)] = \left\langle (\Phi - \langle \Phi \rangle)(\partial_\phi L(\mu|\phi) - \langle \partial_\phi L(\mu|\phi) \rangle) \right\rangle \tag{C.1.2}$$

as $\partial_\phi L(\mu|\phi) = \frac{1}{p(\mu|\phi)}\partial_\phi p(\mu|\phi)$, $\langle\partial_\phi L(\mu|\phi)\rangle = \int \partial_\phi p(\mu|\phi)d\mu = \partial_\phi(\int p(\mu|\phi)d\mu) = 0$ and using definition of unbiased estimator, the above equation reduces to,

$$
\begin{aligned}
&= \langle(\Phi - \phi)(\partial_\phi L(\mu|\phi))\rangle \\
&= \int p(\mu|\phi)\Phi(\mu)\partial_\phi L(\mu|\phi)d\mu \\
&= \int \Phi(\mu)\partial_\phi p(\mu|\phi)d\mu \\
&= \partial_\phi \int \Phi(\mu)p(\mu|\phi)d\mu \\
&= \partial_\phi(\phi) \\
&= 1 \quad\quad\quad\quad\quad\quad\quad\quad\quad\text{(C.1.3)}
\end{aligned}
$$

Now using Cauchy Schwarz inequality for $\Phi(\mu)$ and $\partial_\phi L(\mu|\phi)$, we get

$$
|\langle\Phi - \langle\Phi\rangle, \partial_\phi L(\mu|\phi) - \langle\partial_\phi L(\mu|\phi)\rangle\rangle|^2 \leq \langle(\Phi - \langle\Phi\rangle)^2\rangle\langle(\partial_\phi L(\mu|\phi) - \langle\partial_\phi L(\mu|\phi)\rangle)^2\rangle
$$

The LHS of above eq. is $Cov[\Phi, \partial_\phi L(\mu|\phi)]^2 = 1$,, we get,

$$
1 \leq \Delta^2\Phi\Delta^2\partial_\phi L(\mu|\phi)
$$

as $\Delta^2\partial_\phi L(\mu|\phi) = \langle(\partial_\phi L(\mu|\phi) - \langle\partial_\phi L(\mu|\phi)\rangle)^2\rangle = \langle(\partial_\phi L(\mu|\phi)^2\rangle = F(\phi)$, the above inequality becomes,

$$
\frac{1}{F(\phi)} \leq \Delta^2\Phi \quad\quad\quad\quad\quad\quad\quad\text{(C.1.4)}
$$

For N number of experiments,

$$
\frac{1}{NF(\phi)} \leq \Delta^2\Phi \quad\quad\quad\quad\quad\quad\quad\text{(C.1.5)}
$$

C.2 Expression for SLD

$$
\hat{L}_\phi = 2\sum_{k,l} \frac{(\partial_\phi\hat{\rho}_\phi)_{kl}|k\rangle\langle l|}{p_k + p_l}
$$

Plugging the definition of mixed state i.e., $\hat{\rho}_\phi = \sum_k p_k |\psi_k\rangle\langle\psi_k|$ in eq. (4.1.6) we get,

$$\partial_\phi \hat{\rho}_\phi = \frac{1}{2}\left(\sum_k p_k |\psi_k\rangle\langle\psi_k|\hat{L}_\phi + \hat{L}_\phi \sum_k p_k |\psi_k\rangle\langle\psi_k|\right)$$

introducing identity operator adjacent to SLD, $\hat{1} = \sum_l |\psi_l\rangle\langle\psi_l|$ and writing the matrix elements $\langle\psi_l|\hat{L}_\phi|\psi_k\rangle$ as $(\hat{L}_\phi)_{lk}$,

$$= \frac{1}{2}\left(\sum_{kl} p_k |\psi_k\rangle(\hat{L}_\phi)_{kl}\langle\psi_l| + \sum_{kl} p_k |\psi_l\rangle(\hat{L}_\phi)_{lk}\langle\psi_k|\right)$$

as SLD is hermitian, its eigenvalues are real numbers; therefore, $(\hat{L}_\phi)_{lk} = (\hat{L}_\phi)_{kl}$

$$= \frac{1}{2}\sum_{kl}\left(p_k |\psi_k\rangle\langle\psi_l| + p_k |\psi_l\rangle\langle\psi_k|\right)(\hat{L}_\phi)_{kl}$$

projecting $\langle\psi_i|$ and $|\psi_j\rangle$ from left and right respectively, and using identity $\langle\psi_i|\psi_k\rangle = \delta_{ik}$,

$$(\partial_\phi\hat{\rho}_\phi)_{ij} = \frac{1}{2}\sum_{kl}\left(p_k \delta_{ik}\delta_{lj} + p_k \delta_{il}\delta_{kj}\right)(\hat{L}_\phi)_{ij}$$

$$= \frac{1}{2}(p_i + p_j)(\hat{L}_\phi)_{kl}$$

$(\hat{L}_\phi)_{kl}$ turns out to be,

$$(\hat{L}_\phi)_{ij} = 2\frac{(\partial_\phi\hat{\rho}_\phi)_{ij}}{p_i + p_j}$$

$$\Rightarrow \hat{L}_\phi = 2\sum_{kl}\frac{(\partial_\phi\hat{\rho}_\phi)_{kl}|\psi_k\rangle\langle\psi_l|}{p_k + p_l} \tag{C.2.1}$$

C.3   FI Vs QFI

Taking partial derivative of conditional PDF $p(\mu|\phi)$ with respect to ϕ leads to,

$$\partial_\phi p(\mu|\phi) = Tr(\hat{\Pi}_\mu \partial_\phi\hat{\rho}_\phi)$$

$$= \frac{1}{2}Tr(\hat{\Pi}_\mu \hat{\rho}_\phi \hat{L}_\phi + \hat{\Pi}_\mu \hat{L}_\phi \hat{\rho}_\phi)$$

Using cyclic property of trace and the fact that all the operators involved in above equation are hermitian,

$$= \frac{1}{2} Tr \big[(\hat{\rho}_\phi \hat{\Pi}_\mu \hat{L}_\phi)^\dagger + \hat{\rho}_\phi \hat{\Pi}_\mu \hat{L}_\phi \big]$$

which give way to,

$$= \Re \big[Tr(\hat{\rho}_\phi \hat{\Pi}_\mu \hat{L}_\phi) \big]$$

hence eq. (4.1.3) becomes,

$$F(\phi) = \int d\mu \frac{1}{p(\mu|\phi)} \bigg(\Re \big[Tr(\hat{\rho}_\phi \hat{\Pi}_\mu \hat{L}_\phi) \big] \bigg)^2$$
$$\leq \int d\mu \frac{\big| Tr(\hat{\rho}_\phi \hat{\Pi}_\mu \hat{L}_\phi) \big|^2}{Tr(\hat{\rho}_\phi \hat{\Pi}_\mu)}$$
$$= \int d\mu \frac{\big| Tr(\sqrt{\hat{\rho}_\phi \hat{\Pi}_\mu} \sqrt{\hat{\Pi}_\mu} \hat{L}_\phi \sqrt{\hat{\rho}_\phi}) \big|^2}{Tr(\hat{\rho}_\phi \hat{\Pi}_\mu)}$$

using Cauchy-Schwarz Inequality, $|Tr[\hat{A}^\dagger \hat{B}]|^2 \leq Tr[\hat{A}^\dagger \hat{A}] Tr[\hat{B}^\dagger \hat{B}]$, the above eq. transforms into an inequality given as,

$$\leq \int d\mu Tr[\hat{\Pi}_\mu \hat{L}_\phi \hat{\rho}_\phi \hat{L}_\phi]$$

which through completeness of POVMs yields,

$$= Tr[\hat{L}_\phi \hat{\rho}_\phi \hat{L}_\phi] = Tr[\hat{\rho}_\phi \hat{L}_\phi^2]$$
$$F(\phi) \leq Tr[\hat{\rho}_\phi \hat{L}_\phi^2] \tag{C.3.1}$$

C.4 Unitary QFI

$$F_Q(\hat{\rho}, \hat{G}) = 2 \sum_{kl} \frac{(p_k - p_l)^2}{p_k + p_l} |\hat{G}_{kl}|^2$$

For unitary transformation, the SLD can be written as,

$$\hat{L}_\phi = 2i \sum_{k,l} \frac{\langle \psi_k | [\hat{\rho}_\phi, \hat{G}] | \psi_l \rangle |\psi_k\rangle \langle \psi_l|}{p_k + p_l}$$

where we have used $\partial_\phi \hat{\rho}_\phi = i[\hat{\rho}_\phi, \hat{G}]$, in eq. (C.2.1). Evaluating the commutator leads to,

$$= 2i \sum_{k,l} \frac{p_k - p_l}{p_k + p_l} \hat{G}_{kl} |\psi_k\rangle \langle \psi_l|$$

Squaring SLD gives,

$$\hat{L}_\phi^2 = -4 \sum_{klij} \frac{(p_k - p_l)(p_i - p_j)}{(p_k + p_l)(p_i + p_j)} \hat{G}_{kl}\hat{G}_{ij} |\psi_k\rangle \langle \psi_l|\psi_i\rangle \langle \psi_j|$$

contracting index i gives,

$$= -4 \sum_{klj} \frac{(p_k - p_l)(p_l - p_j)}{(p_k + p_l)(p_l + p_j)} \hat{G}_{kl}\hat{G}_{lj} |\psi_k\rangle \langle \psi_j|.$$

Using definition of QFI,

$$F_Q(\rho, \hat{\phi}) = Tr[\hat{\rho}_\phi \hat{L}_\phi^2]$$

$$= -4 \sum_{iklj} p_i \frac{(p_k - p_l)(p_l - p_j)}{(p_k + p_l)(p_l + p_j)} \hat{G}_{kl}\hat{G}_{lj} \langle \psi_i|\psi_k\rangle \langle \psi_j|\psi_i\rangle$$

$$= -4 \sum_{iklj} p_i \frac{(p_k - p_l)(p_l - p_j)}{(p_k + p_l)(p_l + p_j)} \hat{G}_{kl}\hat{G}_{lj} \delta_{ik}\delta_{ji}$$

contracting index i and j with δ, leads to $j = k$

$$= 4 \sum_{kl} p_k \frac{(p_k - p_l)^2}{(p_k + p_l)^2} |\hat{G}_{kl}|^2$$

$$= 4 \sum_{kl} (1 - \frac{p_l}{p_k + p_l}) \frac{(p_k - p_l)^2}{(p_k + p_l)} |\hat{G}_{kl}|^2$$

$$= 4 \sum_{kl} \frac{(p_k - p_l)^2}{p_k + p_l} |\hat{G}_{kl}|^2 - Tr[\hat{\rho}_\phi \hat{L}_\phi^2]$$

$$= 2 \sum_{kl} \frac{(p_k - p_l)^2}{p_k + p_l} |\hat{G}_{kl}|^2$$

$$F_Q(\hat{\rho}, \hat{G}) = 2 \sum_{kl} \frac{(p_k - p_l)^2}{p_k + p_l} |\hat{G}_{kl}|^2 \tag{C.4.1}$$

C.5   Unitary QFI for Mixed and Pure States

Through simple algebra, QFI for mixed and pure states can be obtained from eq. (C.4.1),

$$F_Q(\hat{\rho}, \hat{G}) = 2 \sum_{kl} \frac{(p_k - p_l)^2}{p_k + p_l} |\hat{G}_{kl}|^2$$

$$= 2 \sum_{kl} \frac{1}{p_k + p_l} (p_k^2 + p_l^2 + 2p_k p_l - 4p_k p_l) |\hat{G}_{kl}|^2$$

$$= 2 \sum_{kl} \left[p_k + p_l - \frac{4p_k p_l}{p_k + p_l} \right] |\hat{G}_{kl}|^2$$

Exploiting the arbitrariness of index l and k, $p_k |\hat{G}_{kl}|^2 = p_l |\hat{G}_{kl}|^2$ which leads to,

$$= 4 \left[\sum_{kl} p_k \langle \psi_k | \hat{G} | \psi_l \rangle \langle \psi_l | \hat{G} | \psi_k \rangle - \sum_{kl} \frac{2p_k p_l}{p_k + p_l} |\hat{G}_{kl}|^2 \right]$$

using completeness of the states $|\psi_l\rangle$

$$= 4 \sum_k p_k \langle \psi_k | \hat{G}^2 | \psi_k \rangle - \sum_{kl} \frac{8p_k p_l}{p_k + p_l} |\hat{G}_{kl}|^2 \tag{C.5.1}$$

For pure state, $\hat{\rho} = |\psi\rangle\langle\psi|$, $p_k = p_l = 1$ for one value of k and l, with rest all as 0. Thus, eq. (C.5.1) becomes

$$= 4\big(\langle\psi|\hat{G}^2|\psi\rangle - \langle\hat{G}\rangle^2\big)$$

$$F_Q(\psi\rangle, \hat{G}) = 4\langle\psi|(\Delta\hat{G})^2|\psi\rangle \tag{C.5.2}$$

For mixed state, using the identity, $Tr[\hat{\rho}(\Delta\hat{G})^2] = \sum_k p_k\langle\psi_k|(\Delta\hat{G})^2|\psi_k\rangle = \sum_k p_k\big[\langle\psi_k|(\hat{G})^2|\psi_k\rangle - |\langle\psi_k|\hat{G}|\psi_k\rangle|^2\big]$ [47] eq. (C.5.1) yields,

$$= 4Tr[\hat{\rho}(\Delta\hat{G})^2] - \left(\sum_{kl}\frac{8p_kp_l}{p_k + p_l}|\hat{G}_{kl}|^2 - 4\sum_k p_k|\langle\psi_k|\hat{G}|\psi_k\rangle|^2\right)$$

$$F_Q(\hat{\rho}, \hat{G}) \leq 4Tr[\hat{\rho}(\Delta\hat{G})^2] \tag{C.5.3}$$

Bibliography

[1] E. Schrödinger, "Die gegenwärtige situation in der quantenmechanik", Naturwissenschaften **23**, 844–849 (1935).

[2] C. Schirm, *English: Schrödinger's cat experiment with propability density of one ear atom.* https://commons.wikimedia.org/wiki/File:Catexperiment.svg, May 2010.

[3] V. Dodonov, I. Malkin, and V. Man'Ko, "Even and odd coherent states and excitations of a singular oscillator", Physica **72**, 597–615 (1974).

[4] M. Brune, S. Haroche, J.-M. Raimond, L. Davidovich, and N. Zagury, "Manipulation of photons in a cavity by dispersive atom-field coupling: quantum-nondemolition measurements and generation of "schrödinger cat"states", Physical Review A **45**, 5193 (1992).

[5] E. P. F. de Lausanne, *Critical Schrödinger Cat Code: Quantum Computing Breakthrough for Better Qubits*, https://scitechdaily.com/critical-schrodinger-cat-code-quantum-computing-breakthrough-for-better-qubits/, June 2023.

[6] C. Monroe, D. M. Meekhof, B. E. King, and D. J. Wineland, "A "schrödinger cat" superposition state of an atom", science **272**, 1131–1136 (1996).

[7] K. Takase, J.-i. Yoshikawa, W. Asavanant, M. Endo, and A. Furusawa, "Generation of optical schrödinger cat states by generalized photon subtraction", Physical Review A **103**, 013710 (2021).

[8] T. Gerrits, S. Glancy, T. S. Clement, B. Calkins, A. E. Lita, A. J. Miller, A. L. Migdall, S. W. Nam, R. P. Mirin, and E. Knill, "Generation of optical coherent-state superpositions by number-resolved photon subtraction from the squeezed vacuum", Physical Review A—Atomic, Molecular, and Optical Physics **82**, 031802 (2010).

[9] A. Ourjoumtsev, H. Jeong, R. Tualle-Brouri, and P. Grangier, "Generation of optical 'schrödinger cats' from photon number states", Nature **448**, 784–786 (2007).

[10] J. S. Neergaard-Nielsen, B. M. Nielsen, C. Hettich, K. Mølmer, and E. S. Polzik, "Generation of a superposition of odd photon number states for quantum information networks", Physical review letters **97**, 083604 (2006).

[11] S. Wang, H.-c. Yuan, and X.-f. Xu, "Conditional generation of fock states and schrödinger-cat states via adding multiple photons to a squeezed vacuum state", The European Physical Journal D **67**, 1–8 (2013).

[12] Z.-H. Li, F. Yu, Z.-Y. Li, M. Al-Amri, and M. S. Zubairy, "Method to deterministically generate large-amplitude optical cat states", Communications Physics **7**, 134 (2024).

[13] S. Haroche, "Nobel lecture: controlling photons in a box and exploring the quantum to classical boundary", Reviews of Modern Physics **85**, 1083–1102 (2013).

[14] D. J. Wineland, "Nobel lecture: superposition, entanglement, and raising schrödinger's cat", Reviews of Modern Physics **85**, 1103–1114 (2013).

[15] J. Hastrup and U. L. Andersen, "All-optical cat-code quantum error correction", Physical Review Research **4**, 043065 (2022).

[16] S.-W. Lee and H. Jeong, "Near-deterministic quantum teleportation and resource-efficient quantum computation using linear optics and hybrid qubits", Physical Review A—Atomic, Molecular, and Optical Physics **87**, 022326 (2013).

[17] A. Gilchrist, K. Nemoto, W. J. Munro, T. C. Ralph, S. Glancy, S. L. Braunstein, and G. J. Milburn, "Schrödinger cats and their power for quantum information processing", Journal of Optics B: Quantum and Semiclassical Optics **6**, S828 (2004).

[18] A. Cao, W. J. Eckner, T. L. Yelin, A. W. Young, S. Jandura, L. Yan, K. Kim, G. Pupillo, J. Ye, N. D. Oppong, et al., "Multi-qubit gates and'schr\" odinger cat'states in an optical clock", arXiv preprint arXiv:2402.16289 (2024).

[19] M. A. Taylor and W. P. Bowen, "Quantum metrology and its application in biology", Physics Reports **615**, Quantum metrology and its application in biology, 1–59 (2016).

[20] C. M. Caves, "Quantum-mechanical noise in an interferometer", Physical Review D **23**, 1693 (1981).

[21] M. A. Taylor and W. P. Bowen, "Quantum metrology and its application in biology", Physics Reports **615**, 1–59 (2016).

[22] N. Shettell and D. Markham, "Quantum metrology with delegated tasks", Physical Review A **106**, 052427 (2022).

[23] W. Ge, K. Jacobs, S. Asiri, M. Foss-Feig, and M. S. Zubairy, "Operational resource theory of nonclassicality via quantum metrology", Physical Review Research **2**, 023400 (2020).

[24] S. Dey, A. Fring, and V. Hussin, "A squeezed review on coherent states and nonclassicality for non-hermitian systems with minimal length", in Coherent states and their applications: a contemporary panorama (Springer, 2018), pp. 209–242.

[25] G. Iwata, "Non-hermitian operators and eigenfunction expansions", Progress of Theoretical Physics **6**, 216–226 (1951).

[26] R. J. Glauber, "Coherent and incoherent states of the radiation field", Physical Review **131**, 2766 (1963).

[27] E. Sudarshan, "Equivalence of semiclassical and quantum mechanical descriptions of statistical light beams", Physical Review Letters **10**, 277 (1963).

[28] K. C. Tan and H. Jeong, "Nonclassical light and metrological power: an introductory review", AVS Quantum Science **1** (2019).

[29] B. Yurke and D. Stoler, "Generating quantum mechanical superpositions of macroscopically distinguishable states via amplitude dispersion", Physical review letters **57**, 13 (1986).

[30] F. Semiao, K. Furuya, and G. Milburn, "Kerr nonlinearities and nonclassical states with superconducting qubits and nanomechanical resonators", Physical Review A—Atomic, Molecular, and Optical Physics **79**, 063811 (2009).

[31] A. Z. Goldberg and K. Heshami, "How squeezed states both maximize and minimize the same notion of quantumness", Physical Review A **104**, 032425 (2021).

[32] B. Lan and X.-x. Xu, "Multi-headed symmetrical superpositions of coherent states", International Journal of Theoretical Physics **61**, 148 (2022).

[33] W. Ge and M. S. Zubairy, "Evaluating single-mode nonclassicality", Physical Review A **102**, 043703 (2020).

[34] J. Francis and M. Tame, "Photon-added coherent states using the continuous-mode formalism", Physical Review A **102**, 043709 (2020).

[35] Z. Dong-Lin and K. Le-Man, "Two-mode excited entangled coherent states and their entanglement properties", Chinese Physics B **18**, 1328 (2009).

[36] A. Zavatta, S. Viciani, and M. Bellini, "Quantum-to-classical transition with single-photon-added coherent states of light", science **306**, 660–662 (2004).

[37] Y.-R. Chen, H.-Y. Hsieh, J. Ning, H.-C. Wu, H. L. Chen, Z.-H. Shi, P. Yang, O. Steuernagel, C.-M. Wu, and R.-K. Lee, "Generation of heralded opticalschroedinger cat'states by photon-addition", arXiv preprint arXiv:2306.13011 (2023).

[38] W. Asavanant, K. Nakashima, Y. Shiozawa, J.-I. Yoshikawa, and A. Furusawa, "Generation of highly pure schrödinger's cat states and real-time quadrature measurements via optical filtering", Optics Express **25**, 32227–32242 (2017).

[39] Y. Shih, "Entangled biphoton source-property and preparation", Reports on Progress in Physics **66**, 1009 (2003).

[40] B. L. Schumaker, "Noise in homodyne detection", Optics letters **9**, 189–191 (1984).

[41] C. C. Gerry and P. L. Knight, *Introductory quantum optics* (Cambridge university press, 2023).

[42] S. Haroche, "Exploring the quantum dynamics of atoms and photons in cavities", in *Quantum coherence in solid state systems* (IOS Press, 2009), pp. 1–13.

[43] L. Mandel, "Sub-poissonian photon statistics in resonance fluorescence", Optics letters **4**, 205–207 (1979).

[44] *Super-Poisson*, https://liorpachter.wordpress.com/tag/super-poisson/.

[45] M. A. Nielsen and I. L. Chuang, *Quantum computation and quantum information* (Cambridge university press, 2010).

[46] M. G. Paris, "Quantum estimation for quantum technology", International Journal of Quantum Information **7**, 125–137 (2009).

[47] G. Tóth and D. Petz, "Extremal properties of the variance and the quantum fisher information", Physical Review A—Atomic, Molecular, and Optical Physics **87**, 032324 (2013).

[48] G. Tóth and I. Apellaniz, "Quantum metrology from a quantum information science perspective", Journal of Physics A: Mathematical and Theoretical **47**, 424006 (2014).

[49]K. C. Tan, T. Volkoff, H. Kwon, and H. Jeong, "Quantifying the coherence between coherent states", Physical review letters **119**, 190405 (2017).